



**CERN-ACC-NOTE-2018-0078**

2018-11-23

fredrik.wenander@cern.ch

## **Summary of charge breeding investigations for a future $^{11}\text{C}$ treatment facility**

**Authors:** J. Pitters, M. Breitenfeldt, H. Pahl, A. Pikin and F. Wenander

**Keywords:** cancer therapy, carbon ion, charge breeding, EBIS, Penning trap

---

### **Abstract**

In this report we discuss the possibilities of using a charge breeding scheme based on an Electron Beam Ion Source for beam preparation of a radioactive  $^{11}\text{C}$  beam for hadron therapy. Test measurements under extreme operating conditions were conducted at the REX-ISOLDE facility to explore the limitations of the charge breeder for high-intensity, low-repetition-rate, molecular  $\text{CO}^+$  beams. Based on our findings, we discuss different possible scenarios of coupling a charge breeder with either a medical synchrotron or linear accelerator.

---

# Summary of charge breeding investigations for a future $^{11}\text{C}$ treatment facility

J. Pitters<sup>1</sup>, M. Breitenfeldt<sup>2</sup>, H. Pahl<sup>1,3</sup>, A. Pikin<sup>1,4</sup>, F. Wenander<sup>1</sup>

<sup>1</sup> CERN, Route de Meyrin, 1211 Geneva 23, Switzerland

<sup>2</sup> ADAM SA, Rue de Veyrot 11, 1217 Meyrin, Switzerland

<sup>3</sup> Heidelberg Graduate School of Fundamental Physics, Heidelberg University,  
Im Neuenheimer Feld 226, 69120 Heidelberg, Germany

<sup>4</sup> School of Physics and Astronomy, The University of Manchester, Manchester,  
M13 9PL, United Kingdom

## Abstract

In this report we discuss the possibilities of using a charge breeding scheme based on an Electron Beam Ion Source for beam preparation of a radioactive  $^{11}\text{C}$  beam for hadron therapy. Test measurements under extreme operating conditions were conducted at the REX-ISOLDE facility to explore the limitations of the charge breeder for high-intensity, low-repetition-rate, molecular  $\text{CO}^+$  beams. Based on our findings, we discuss different possible scenarios of coupling a charge breeder with either a medical synchrotron or linear accelerator.

## 1 Introduction

Within work-package 2 of the MEDICIS-Promed ITN [1,2], we study the possibilities of using a radioactive ion beam in hadron therapy. In particular,  $^{11}\text{C}$  ( $\beta^+$  emitter,  $T_{1/2} = 20.4$  min) is investigated as it has excellent properties for both on-line and off-line PET imaging, which can be used for dose verification [3]. While ions are produced abundantly in conventional hadron therapy with stable carbon, it is highly challenging to provide a radioactive beam of adequate intensity for treatment. We have initially focused on an acceleration scheme based on a synchrotron, as described in the Proton Ion Medical Machine Study (PIMMS) [4,5] and used presently at CNAO (Pavia, Italy) [6] and at MedAustron (Wiener Neustadt, Austria) [7]. This was requested by the MEDICIS-Promed steering committee, as an essential step would be to try out treatment with  $^{11}\text{C}$  ions at one of these facilities. Furthermore, it shall be assumed that the radioactive treatment ions are produced by the Isotope Separation On-Line (ISOL) technique [8]. Previous experience with carbon ion beams at the nuclear physics facility ISOLDE [9] at CERN has shown that the  $^{11}\text{C}$  output with the highest yield from the ISOL-production stage is typically a singly charged, molecular  $^{11}\text{CO}^+$  beam [10]. Molecular carbon in form of CO is volatile and can therefore be extracted from the target with higher yields than atomic carbon, that is refractory and easily forms strong bonds with hot metal surfaces. The main challenge of the

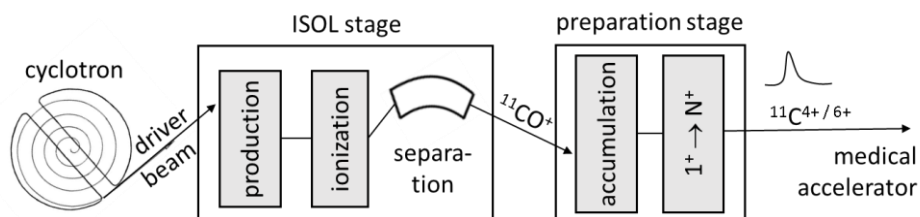


Figure 1. Schematic layout of an ISOL-production and preparation stage for  $^{11}\text{C}^+$  to be used as treatment beam in a synchrotron-based facility.

work discussed in this report lies in coupling the production of a continuous, molecular  $\text{CO}^+$  beam from an ISOL-target with a low repetition-rate medical accelerator (see Figure 1).

The concept of accumulation, breeding and post-acceleration of radioactive carbon beams was tested at REX-ISOLDE [11,12], which is part of ISOLDE. Here, ISOL-produced radioactive beams are prepared in a charge-breeding stage (see Figure 2) before acceleration in the HIE-ISOLDE linac [13] and further transfer to the experimental stations. The charge breeding stage consists of two main devices, namely a Penning trap and an Electron Beam Ion Source (EBIS). The Penning trap, REXTRAP [14,15], cools and bunches the quasi-continuous beam from ISOLDE. The bunched beam is transported via an electrostatic transfer section and injected into REXEBIS [16,17], where the ions' charge state of initially  $1^+$  is increased for an efficient post acceleration. After separation by A/Q in a Nier-type spectrometer [18], the selected beam is accelerated in the HIE-ISOLDE linac.

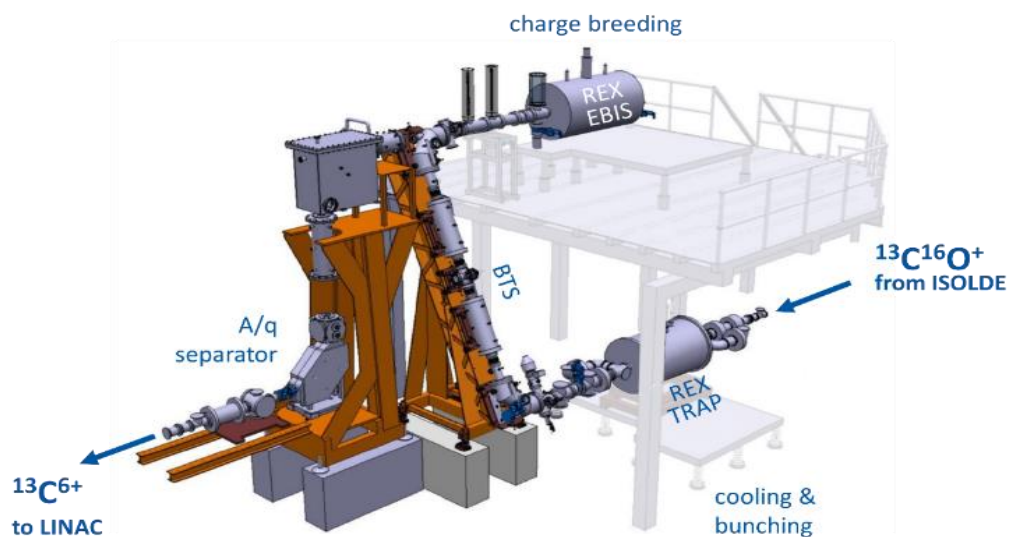


Figure 2. REX-ISOLDE low energy stage, comprised of REXTRAP for cooling and bunching of the  $1^+$  ion beam, the electrostatic beam transfer section (BTS), REXEBIS for charge breeding  $1^+ \rightarrow N^+$  and an A/Q separator. The charge breeder stage transforms a continuous  $1^+$  beam into a pulsed beam of higher charge.

At ISOLDE, the efficiency of the charge breeder stage, comprised of REXTRAP, REXEBIS and the spectrometer, is of major concern. Typically, rare isotopes with small production cross-sections are handled, hence, ion intensities are relatively low (ranging from a few ions/s to  $>10^8$  ions/s). In contrast to ISOLDE, a beam preparation stage for hadron therapy has to deal with considerably higher intensities. The efficiency will still play a central role in the design, as the production of the radioactive ions is limited. Furthermore, a synchrotron-based treatment facility would require long storage times of the  $1^+$  ions, which is an additional challenge. For the tests presented here, the REX-ISOLDE charge breeder stage had to be operated well outside the normal regime to determine its limitations in the context of hadron therapy.

In this report, different possibilities of using a charge breeding stage as a CO beam preparation tool for hadron therapy with a synchrotron are laid out and investigated with regard to their feasibility and technical limitations. Firstly, basic properties of a charge breeder stage are discussed by reference to the setup at REX-ISOLDE. Secondly, measurement data taken at ISOLDE is presented that quantifies the behaviour and limitations of the Penning trap and EBIS under the extreme conditions of high-intensity, low repetition-rate beams. Thereby, various injection scenarios that correspond to different design options for a hadron therapy beam preparation stage are compared.

As this study pinpoints the difficulty of efficiently coupling an  $^{11}\text{C}^+$  beam from an ISOL-stage with a synchrotron based accelerator, a green field approach is presented, that discusses possibilities of matching the radioactive beam with future medical accelerators, in particular with a high-repetition-rate, all-linac system.

## 2 Charge breeding requirements and components

### 2.1 Charge breeding requirements for a synchrotron based facility

In conventional carbon ion therapy facilities, the stable beam is produced in an Electron Cyclotron Resonance (ECR) ion source, with continuous currents of several 100  $\mu\text{A}$ . Beam can be injected into the synchrotron only during some tens of  $\mu\text{s}$  at the beginning of each cycle. Since stable carbon is available abundantly, one can afford to chop the beam extracted from the ECR ion source and inject a pulse of the desired length into the synchrotron, while discarding >99.99 % of the initially produced beam. However, in case of a radioactive treatment beam, the limited production rate of the radioisotopes imposes the need of ion accumulation during the length of one synchrotron cycle (>1 s), in order to reach the desired intensity. For light ions as carbon, the ECR ion source has very limited storing capability and it is therefore not suitable as a stand-alone source for the radioactive beam. Instead, a charge breeding stage with a storing capability is required.

Typically, an EBIS-based charge breeding system operates with a repetition rate between 2 and 50 Hz [17]. Thus, the low repetition rate of the synchrotron (<1 Hz) enforces a challenge on the design of the charge breeder system, to effectively match the quasi-continuous  $1^+$  ion beam from the target ion-source with a synchrotron. The output of the charge breeder should ideally be a pulse of carbon ions of charge state  $4^+$  or higher, with a pulse length that can be accepted for injection into the synchrotron, i.e. some tens of  $\mu\text{s}$ . If longer pulses are provided, the efficiency of the multi-turn injection decreases. According to the PIMMS design report [5], the required intensity of beam out of the ECR ion source is  $5.6 \cdot 10^9$   $\text{C}^{4+}$  ions per pulse (pulse length of 30  $\mu\text{s}$ , corresponding to an injection over 16 synchrotron turns in the PIMMS design). This number is to be understood as a lower limit as higher intensities may be required to compensate for losses in a real machine. To include a safety margin, we have aimed at  $1 \cdot 10^{10}$  ions per pulse, which would also be sufficient to complete a treatment in one single synchrotron spill, given that the rest of the machine is relatively efficient.

Functions of the charge breeder system	Details
Accumulation of CO beam	During >1 s
Molecular breakup	CO $\rightarrow$ C + O
Charge breeding	$\text{C}^{4+}$ , $\text{C}^{5+}$ or $\text{C}^{6+}$
Extracted pulse length	<100 $\mu\text{s}$
Output intensity	$1 \cdot 10^{10}$ ions
Maximum emittance for $\text{C}^{4+}$ , 95% at 30 kV [19]	Approx. 180 mm mrad

*Table 1. Summary of the required functions of the charge breeding system for a hadron therapy facility based on a synchrotron.*

### 2.2 Electron Beam Ion Source

The central part of the charge breeder system is an EBIS. Here, the main working principles of an EBIS are described and important terms which are used in the discussion later are defined. For a more detailed description of the EBIS and its functionality, the reader is referred to the literature [20,21].

#### 2.2.1 Electron beam

Inside an EBIS, an electron beam is generated by an electron gun. The electron beam is injected into a solenoidal magnetic field that compresses it to reach a high current density. On the other side of the

magnet, it is recovered on the collector electrode. In REXEBIS, for example, a 200 mA electron beam of 4.5 keV is transported over a trap length of 0.8 m. Inside the 2 T solenoidal field, the beam is compressed down to a radius of 250  $\mu\text{m}$ , resulting in an electron current density of approximately 100 A/cm<sup>2</sup>.

### 2.2.2 EBIS cycle

In the EBIS, highly charged ions are produced by electron impact ionization. They can either be introduced as neutral gas or injected from an external source as 1<sup>+</sup> ions and thereafter charge bred in the electron beam. At REX, under normal operating conditions, the 1<sup>+</sup> beam is bunched in REXTRAP prior to injection into the EBIS. In every EBIS cycle, the injection barrier, created by the potential on one of the outer drift tubes, is lowered during injection and an ion bunch from the Penning trap is injected. Before the ions perform one complete axial roundtrip inside the EBIS, the injection barrier is closed again to trap the ions before they can escape the EBIS. The ions are now radially confined by the space charge potential of the electron beam and axially by the electrostatic barriers. During the time the ions spend in the ionization region, called breeding time, an ion's charge state evolves due to the exposure to competing atomic processes: electron impact ionization, radiative and di-electronic recombination, and charge exchange [22]. At the end of the cycle, when the ions are extracted by again lowering the barrier, a certain charge state distribution (CSD) has been established which is mainly determined by the breeding time and the electron beam density. Downstream from the EBIS, a specific charge state can be selected by means of an electromagnetic spectrometer.

### 2.2.3 Capacity

The charge storage capacity of the EBIS is given by the total space charge of the electrons within the trapping length L. The number of electrons can be approximately calculated from the non-relativistic electron energy E<sub>e</sub> and the beam current I<sub>e</sub>:

$$N^- = \frac{L \cdot I_e}{e} \cdot \sqrt{\frac{m_e}{2E_e}} \quad (1)$$

with e and m<sub>e</sub> being the electron charge and mass, respectively. In REXEBIS, with I<sub>e</sub>=200 mA, E<sub>e</sub>=4.5 e·kV and L=0.8 m, the total electron number amounts to 2.3·10<sup>10</sup> electrons.

A low beam energy is favourable if the trapping capacity has to be maximized. However, from an electron optics point of view, a lower beam energy is more difficult to handle, and a trade-off must be made. The electron energy also determines the maximum attainable charge state of the ions. This, however, is not of concern for this particular application, as carbon is a light ion and can easily be ionized – with a threshold energy of 490 eV to go from C<sup>5+</sup> to C<sup>6+</sup>. Significantly higher electron beam energies are only required for charge breeding of heavy ions to high charge states.

### 2.2.4 Radial trapping potential and neutralization

The radial trapping potential is created by the space charge of the electrons. Assuming a uniform distribution of the electrons inside the electron beam radius r<sub>e</sub>, the potential inside the drift tubes (radius r<sub>d</sub>) takes the following form.

$$U(r) = \frac{(1-k) \cdot I_e}{4\pi\epsilon_0 \sqrt{\frac{2E_e}{m_e}}} \begin{cases} \left( -1 + 2 \ln \left( \frac{r_e}{r_d} \right) + \left( \frac{r}{r_e} \right)^2 \right) & r \leq r_e \\ 2 \ln \left( \frac{r}{r_d} \right) & r_e < r \leq r_d \end{cases} \quad (2)$$

Here,  $\epsilon_0$  is the vacuum permittivity and k is the neutralization factor, which describes the filling of the electrons' space charge potential. It is defined as the ratio of ion charges to electron charges inside the trapping volume of the EBIS. When the EBIS is filled with ions, the electron space charge becomes

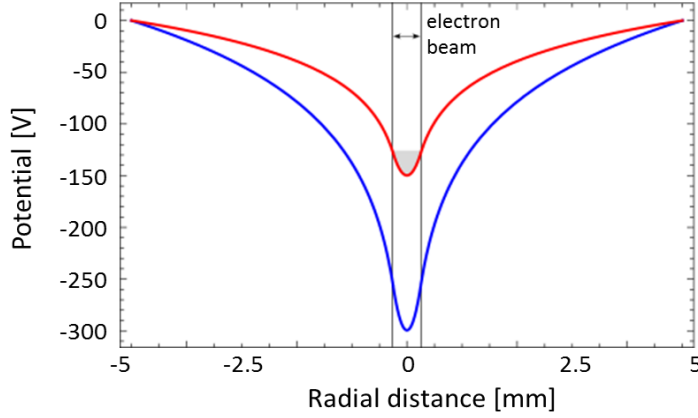


Figure 3. Radial space charge potential relative to the drift tubes inside REXEBIS in the absence of ions (blue) and partially neutralized,  $k=0.5$  (red).

neutralized according to the neutralization factor  $k$  and the potential well becomes less deep. Figure 3 shows the space charge potential of the REXEBIS electron beam with partial and without neutralization by ions.

When estimating the number of carbon ions the EBIS can hold, one has to take into account that the EBIS can not be filled completely ( $k < 1$ ), as will be discussed below, and that the fraction of the capacity that is actually used, is distributed over different elements (residual gases and injected ions) and charge states. The number of ions of element  $X$  in charge state  $Q$  is:

$$N_X^{Q+} = \frac{k \cdot N^- \cdot \delta_X \cdot f_X^Q}{\sum_{\text{elements} < Q > \cdot \delta} \quad (3)$$

with  $\delta_X$  being the fraction of particles of element  $X$ ,  $f_X^Q$  the fraction of particles in charge state  $Q$  of element  $X$ , and  $\langle Q \rangle$  the average charge state of element  $X$ . Typically, the background from residual gas amounts to  $10^8$  to  $10^9$  charges per pulse at REXEBIS, meaning that residual gas ions fill the electron beam by up to 5%. The main contribution to this background is Ne, coming from the REXTRAP buffer gas. If no buffer gas is injected into the Penning trap, the background neutralization can be  $< 1\%$ .

### 2.2.5 Ion losses from boil-off

An important ion loss mechanism in the EBIS is thermal boil-off [23]. Ions are heated by Spitzer collisions [24,25] with the fast electrons, and gain energy from so-called ionisation heating when they change charge state within the electron beam potential. Inside the electron beam, different ion populations thermalize within some milliseconds until their energies follow a Maxwell-Boltzmann distribution in the radial and axial dimensions. Hot ions in the high-energy tail of the distribution are lost if they exceed a certain energy threshold. In the radial trapping dimension, ions have too large radii and hit the drift tubes if their energy exceeds the depth of the radial trapping potential, given by Eq. 2. In the axial direction, ions boil off over the outer barrier, where the energy threshold is determined by the potential difference of the outer barrier and the trapping tubes. This loss mechanism becomes particularly important for long storing times in the EBIS, and for cases where the  $1^+$  ions are injected with a high energy, as the boil-off is more likely for ions with relatively high energies (see Sec. 3.4).

### 2.2.6 Transverse acceptance

The total normalized acceptance  $\alpha_{\text{full}}$  of the EBIS for injected beam is given by the potential depth and radius of the electron beam and can be estimated using the following equation [16]:

$$\alpha_{norm} = \frac{r_{e,trap}}{c} \sqrt{2 \cdot \Delta U_{e,trap} \cdot q/m}, \quad (4)$$

where  $r_{e,trap}$  and  $\Delta U_{e,trap}$  represent electron beam radius and potential depth,  $c$  the speed of light, and  $q$  and  $m$  ion charge and mass. The formula neglects the contribution from the solenoidal magnetic field, which is adequate as the electrostatic contribution to the acceptance is dominating when the compensation degree is low (as is the case during  $1^+$  ion injection). An EBIS with an electron beam radius  $r_{e,trap}$  of 0.8 mm and a potential depth  $\Delta U_{e,trap}$  inside the electron beam of approximately 1 kV - similar parameters to RHIC-EBIS - would have a normalized acceptance of 0.36 mm mrad for a  $^{11}\text{C}^+$  beam.

### 2.3 Penning trap

Before the ions are injected into REXEBIS, the radioactive ions from the ISOLDE target are cooled and bunched in REXTRAP. The ion accumulation interval followed by the short ion extraction phase make up the so-called period time. The device is a buffer-gas filled (usually Ne) Penning trap built into a 3 T superconducting solenoid. In normal operation the ions enter the trap with a residual kinetic energy of around 200 eV and are stopped in the buffer gas. The central electrode is split azimuthally and a transverse RF-field can be applied for mass-selective cooling of the ions. At REXTRAP, quadrupolar sideband and rotating wall cooling are implemented [15,26]. Normally, the rotating wall mode is used as it yields the highest transmission.

The Brillouin limit determines the maximum attainable density which depends on the magnetic field  $B$  and ion mass  $m$  [27]:

$$\frac{N^+}{V_{cloud}} = \frac{\epsilon_0 B^2}{2m} \quad (5)$$

with  $N^+$  the number of stored charges and  $V_{cloud}$  the ion cloud volume. For  $^{13}\text{CO}^+$  the Brillouin limit lies at  $8.2 \cdot 10^8$  ions/cm<sup>3</sup> and the maximum space charge capacity can therefore be calculated from the cloud volume. Unfortunately, in our setup, the cloud size cannot be determined directly. However, taking the REXTRAP geometry and cloud shape (see a detailed discussion in e.g. [15,26]) into account, 0.5 cm<sup>3</sup> is a reasonable value, which would result in  $4 \cdot 10^8$   $^{13}\text{CO}^+$  ions.

Theoretically, the Brillouin density can be reached when the cloud rotates at  $\frac{\omega_c}{2}$ , i.e. half of the true cyclotron frequency  $\omega_c = qB/m_{ion}$ . When centring the ion cloud with rotating wall cooling, this motion can be driven by applying the cyclotron frequency to the 8-fold segmented ring electrode located at the trap centre, with a phase shift of 90° between neighbouring electrodes. Tests at REXTRAP have shown that due to the presence of the buffer gas and trap imperfections, the RF centring mechanism is most probably not dominated by rotating wall cooling, but by the conventional sideband cooling. Hence, it has to be assumed that the maximum plasma density might not be reached and that saturation effects may occur below the theoretical Brillouin limit.

The trap transmission is defined as the ratio of the  $1^+$  ion beam currents before and after the trap. During typical operation at 2-50 Hz, the trap transmission for a singly charged, mono-atomic beam ranges between 30% and 70%; the lower value occurring for very light ions ( $A < 15$ ). Losses happen mainly upon injection into the trap when ions enter the trapping region over an electrostatic barrier. During their first round-trip inside the trapping region, they have to lose enough energy not to escape over the injection barrier on the way back. If the cooling is insufficient and their energy is still higher than the barrier, the ions will not be trapped. In addition, ions with angles outside of the acceptance cone of the magnetic mirror will be reflected before entering the actual trapping region.

Efficiency refers to the fraction of beam that can actually be accepted by the EBIS. Beam that is not completely cooled may exit the trap and contribute to the transmitted current, even though it does not lie within the EBIS acceptance and is lost during beam transport or upon injection into the EBIS. In particular, this is the case when several masses are present in the trap. The sideband cooling is mass-selective, meaning that only one mass can be cooled efficiently. Other masses may be transmitted through the trap but cannot be injected into the EBIS efficiently.

### 3 Measurements at REX-ISOLDE

The measurements described in this section aim to understand the limits of the charge breeder system when handling high intensities, long accumulation times and molecular beams. The measurements quantify the space charge limits and loss mechanisms due to long ion holding times under different operating conditions of the Penning trap and EBIS. Furthermore, the breakup of CO was studied for different trap configurations and buffer gases. All measurements were performed with stable beams, either from the ISOLDE General Purpose Separator GPS [28], or from the local off-line surface ion source in front of the Penning trap (only K, not CO) [29].  $^{13}\text{CO}^+$  beams were produced in an ISOLDE target ion-source unit by injecting  $^{13}\text{CO}$  gas into a Versatile Arc Discharge Ion Source VADIS [30] via a leak. The measurements were performed with stable  $^{13}\text{CO}^+$  as radioactive  $^{11}\text{CO}^+$  beams with sufficient intensities cannot be reached with the present ISOL-system, and for the more abundant  $^{12}\text{CO}$ ,  $^{12}\text{C}$  suffers from high background levels after mass separation, particularly from oxygen. It is assumed that the behaviour of the radioactive ions is similar to that of the stable beam. For a radioactive beam, slightly higher loss rates in the Penning trap are expected due to the radioactive decay. However, as the half-life of  $^{11}\text{C}$  is relatively long ( $T_{1/2} = 20.4$  min), only a small fraction of the ions decays during the storing time in the trap (decay constant  $5.7 \cdot 10^{-4} \text{ s}^{-1}$ ). Concerning the space charge limitation, the results for the Penning trap can be scaled with the mass difference according to Eq. 5. In the EBIS no difference in capacity is expected between radioactive and stable beam as it depends only on the charge and not on the mass of the ions, to the first order.

#### 3.1 CO injection into REXTRAP

##### 3.1.1 Molecular breakup

When injecting  $\text{CO}^+$  into REXTRAP, the molecule might break up into carbon and oxygen. In principle, the CO molecule has to be broken up at some point in the charge breeding system. Therefore, it would actually be favourable if all molecules could be broken up in the trap such that all oxygen can be removed and an ion beam of atomic carbon is injected into the EBIS, thereby reducing the occupied space charge in the EBIS. The problem, however, is that when the  $\text{CO}^+$  dissociates in the trap, it is not guaranteed that the carbon atom remains positively charged. In the breakup there are two possible exit channels [31]:

- $\text{CO}^+ \rightarrow \text{C}^+ + \text{O}$  (neutral)
- $\text{CO}^+ \rightarrow \text{C}$  (neutral) +  $\text{O}^+$ ,

where the branching ratio depends, among other things, on the collision energy with the neutral atom, with higher energies leading to an increased  $\text{O}^+/\text{C}^+$  ratio [31]. In the second channel, the carbon atom is neutralized and lost. When breakup happens, three beam components can exit the Penning trap:  $\text{C}^+$ ,  $\text{O}^+$  and  $\text{CO}^+$ . In addition, there might be a background from ions that are produced in the trap. The beam transfer section (BTS) from the Penning trap to the EBIS is completely electrostatic, so all beams can be transferred to the EBIS, but they will have different flight times. As will be seen below, the difference in time-of-flight (TOF) between the  $^{13}\text{C}^+$  and  $^{13}\text{CO}^+$  is approximately 13  $\mu\text{s}$  at the measurement position after the Penning trap. Until the EBIS entrance, they travel another distance of approximately 8 m at 30 keV, hence, they will be separated by 19  $\mu\text{s}$  in total. This time difference is



shorter than the roundtrip time inside the EBIS trapping region for the fastest ion (35-40  $\mu\text{s}$  for  $\text{C}^+$ ). It is therefore expected that all three beams can be accepted by the EBIS during the injection window.

In the buffer gas, energy is transferred between the injected beam and the neutral buffer gas atoms through collisions. If the energy in the centre-of-mass frame of the collision exceeds the dissociation energy of the molecule, there is a possibility that the molecule breaks up, which might lead to carbon losses. In tests with molecular  $\text{CO}^+$  beams in REXTRAP, the influence of different parameters such as the injection energy, cooling time and choice of buffer gas on the trapping efficiency and breakup were investigated. Here, injection energy is defined as the potential energy of the ions relative to the REXTRAP platform (0 V in Figure 4).

For ion energies in the eV to keV range, nuclear stopping dominates over electronic stopping and the process can be described by elastic collisions of the ions with the buffer gas atoms [32]. Within the kinematic model of buffer gas cooling, ions and buffer gas atoms are modelled as hard spheres. It is assumed that the diameter of these spheres is to first order proportional to the respective mass. The energy threshold for breakup is where the ion's energy in the centre-of-mass frame of the collision reaches the dissociation energy. This threshold energy has to be compared to the maximum energy transfer in a head-on collision (zero impact parameter). Eq. 6 translates the ion's kinetic energy in the laboratory frame  $E_{\text{lab}}$  into the centre-of-mass frame of the collision  $E_{\text{CM}}$ , depending on the ion and buffer gas masses,  $m_{\text{ion}}$  and  $m_{\text{b}}$ .

$$E_{\text{CM}} = \frac{m_{\text{b}}}{m_{\text{ion}} + m_{\text{b}}} E_{\text{lab}} \quad (6)$$

In lighter buffer gases, the energy transfer per collision is lower than in heavy gases, hence the molecules are less likely to break up. On the other hand, the cooling times, in REXTRAP typically in the order of some 10 ms, are longer than in heavier gases as more collisions are required to stop the ion.

The  $\text{CO}^+$  molecule ( $A=29$ ) is bound with a threshold dissociation energy of 8.3 eV [31]. For the buffer gases He ( $A=4$ ) and Ne ( $A=20$ ), Eq. 6 yields threshold injection energies as listed in Table 2.

Buffer gas	Threshold energy $E_{\text{lab}}$
He	68.5 eV
Ne	20.3 eV

Table 2. Threshold energies for breakup of a  $^{13}\text{C}^{16}\text{O}^+$  molecule in different buffer gases, assuming a dissociation energy of 8.3 eV.

The threshold is the energy at which breakup is possible for head-on collisions. However, the impact parameter is randomly distributed and most molecules will survive an injection also with an energy above the threshold. Nevertheless, if the differential pumping is insufficient, breakup is also possible at an injection energy below the threshold, as buffer gas that exits the trapping region can cause breakup at the trap entrance, where the ions still have a higher energy. A second reason for an effectively lower threshold would be if the molecules can be broken up through a stepwise excitation over several interactions with the buffer gas.

Figure 4 shows different configurations of the axial trapping potential in REXTRAP. In the normal trap configuration (black) the ions enter the trap over the injection barrier with around 200 eV compared to the trap centre, as indicated by the arrow. The ions oscillate in the axial potential well and are gradually stopped by collisions with the Ne buffer gas. Once the ions have migrated to the trap centre, the RF that is applied to the segmented, central trap electrode, couples the magnetron and reduced cyclotron motions, which, in the presence of a buffer gas, has a radial centring effect on the ions.

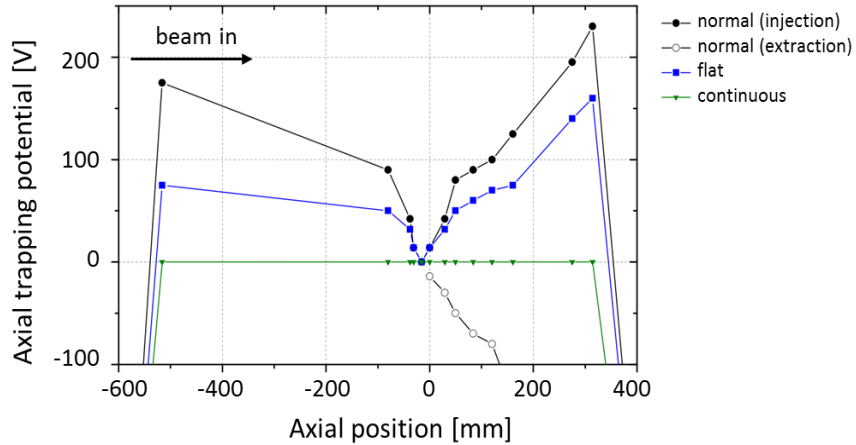


Figure 4. Different configurations of the axial trapping potential in REXTRAP. In the normal trapping configuration, the beam enters from the left side several 10 eV above the barrier or approximately 200 eV above the central trapping electrode.

The normal trap configuration with an injection energy of 200 eV is usually used for atomic beams. When injecting  $\text{CO}^+$ , a significant fraction of the beam breaks up, which is not surprising given the threshold of 20.3 eV. Most of the extracted beam is atomic carbon ions, with possibly some oxygen in the peak. It has to be assumed that for every oxygen ion coming out of the trap, one carbon atom was lost. In an attempt to avoid the dissociation of the  $\text{CO}^+$  molecules, we lowered the injection energy. The axial trapping potential was changed according to the potential shown in Figure 4, referred to as the ‘flat’ trap. As the injection barrier is lower, the whole trap platform potential could be increased by 100 V, thereby effectively lowering the ion injection energy by 100 eV. Indeed, it could be shown that the beam is less prone to breakup in this configuration.

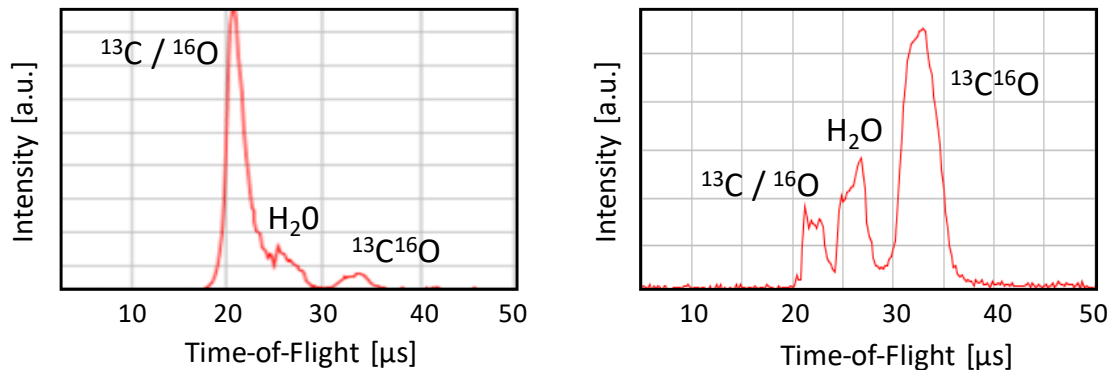


Figure 5. TOF spectra after REXTRAP when using Ne as buffer gas. A  $^{13}\text{C}^{16}\text{O}^+$  beam is injected into the normal trap (left plot: cooling RF tuned for  $A=13$ , period time = 100 ms, injected current 41 pA) and into a flat trap configuration (right plot: cooling RF tuned for  $A=29$ , period time = 41 ms, injected current 57 pA) [30]. Note that the peak identification in [30] is incorrect.

The three different beam components,  $\text{C}^+ / \text{O}^+$  (mainly  $\text{C}^+$  with possibly some  $\text{O}^+$ ),  $\text{H}_2\text{O}^+$  (background contamination from the Penning trap) and  $\text{CO}^+$ , are identified by a time-of-flight measurement directly after the trap. The TOF spectra corresponding to the beam out of the normal and the flat trap configurations are given in Figure 5. Note that the intensities in the two plots cannot be compared, only the relative heights of the peaks are meaningful. The TOF for the flat trap had a lower extracted current. The trap cooling RF was different in the two measurements: in the normal trap C was enhanced by cooling on  $A=13$ , while  $\text{CO}^+$  ( $A=29$ ) was cooled in the flat trap. In the TOF spectrum, the cooling increases the output of the corresponding mass in the order of 10%. This effect might seem

only like a small improvement, however, when injecting into the EBIS, the efficiency for the cooled mass will be a factor 2 to 4 higher than for a non-cooled beam. By lowering the injection energy, the TOF measurements clearly indicated less molecular breakup in the flat trap.

The measurements shown in Figure 5 were taken for a period time of  $\leq 100$  ms. For a CO charge breeding system connected to a synchrotron, longer period times are expected. We have therefore repeated the TOF measurement for different period times as shown in Figure 6. The injection was gated such that always the same amount of ions, namely  $1.24 \cdot 10^8$   $\text{CO}^+$ , were injected during the first 100 ms of the cycle. Even though the total intensities decrease for longer period times due to losses (see Sec. 3.1.2), Figure 6 shows that the relative intensities of the  $\text{C}^+ / \text{O}^+$ ,  $\text{H}_2\text{O}^+$  and  $\text{CO}^+$  peaks do not change significantly. It can therefore be concluded that the breakup happens mainly upon injection into the buffer gas and is not related to the applied RF from the central trapping electrode during the cooling period.

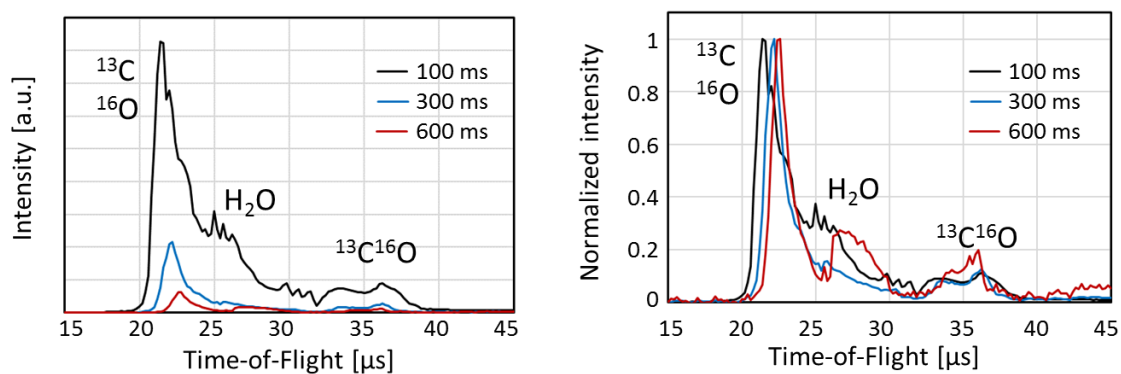


Figure 6. TOF spectra (to the right normalized) after REXTRAP filled with Ne buffer gas and operated in normal trapping configuration, while cooling on mass 13. A total of  $1.24 \cdot 10^8$   $^{13}\text{C}^{16}\text{O}^+$  ions are injected during the first 100 ms of each cycle and thereafter held for different times. As the relative peak heights do not change significantly for long holding times, we conclude that the breakup happens solely during injection and not during RF cooling.

When changing the buffer gas to He, one expects a higher threshold for collisional breakup from the kinematic model of buffer gas cooling. As already listed in Table 2, the threshold for breakup of  $\text{CO}^+$  in He lies at 68.5 eV injection energy, compared to 20.3 eV in Ne. Above we have shown that lowering the injection energy in Ne from 200 to 100 eV, still about 80 eV above the threshold, results in a significant reduction of molecular breakup. Hence, it is expected that an even larger fraction of  $\text{CO}^+$  molecules survives, when injecting  $\text{CO}^+$  into a He-filled trap. Figure 7 presents the TOF spectrum after the Penning trap, when filled with He buffer gas. For this measurement, the trapping potential was again in a flat configuration, as we were trying not to break up the molecule, and the cooling RF tuned for  $\text{CO}^+$ . The trap period time was 50 ms and the total trap transmission only 16%. The actual efficiency was even lower as a large fraction of the extracted beam consisted of  $\text{H}_2\text{O}^+$ . Indeed, from the kinematic model, a lower injection efficiency is expected in He, compared to a similar situation in Ne, as the cooling is slower due to the lower energy transfer per collision. Hence, more ions will escape over the barrier because they have not been sufficiently cooled during their first round-trip in the Penning trap.

When using He as buffer gas, no trace of a  $\text{C}^+ / \text{O}^+$  peak was observed in the TOF spectrum. Hence, the number of broken-up molecules is assumed to be reduced, in agreement with the collisional model. In addition to the data shown above, we have also injected  $\text{CO}_2^+$  into the trap with the same result: the transmission in He is lower than in Ne and the  $\text{C}^+ / \text{O}^+$  peak completely disappears. Due to the significantly lower over-all efficiency, the idea of using He as buffer gas was discarded. All measurements presented below were taken with Ne as buffer gas.

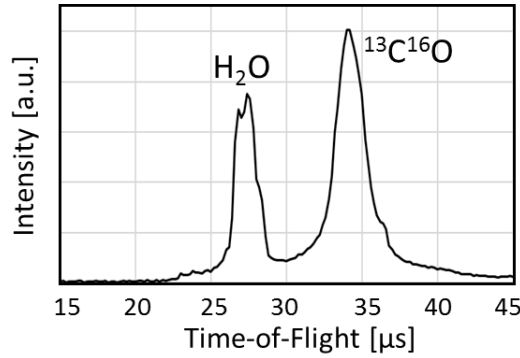


Figure 7. TOF spectra after REXTRAP filled with He buffer gas in a flat trapping configuration, cooling on  $A=29$ . The  $C^+ / O^+$  peak vanishes due to reduced number of break-ups.

### 3.1.2 CO losses during long holding times in REXTRAP

For the  $^{13}\text{C}$  charge breeding system, long accumulation times, in the order of 1 s and longer, are required to store the continuously produced ions between synchrotron cycles. Already during tests with low intensity beams, a reduced transmission through REXTRAP for  $\text{CO}^+$  was recorded when the period time was increased. To quantify the effect, a dedicated test with beams from the ISOLDE target was performed, where the losses related to the long holding time, that resemble an exponential decay of the ion population, were quantified. This loss behaviour of different beams, namely  $\text{CO}^+$ ,  $\text{C}^+$ ,  $\text{Be}^+$  and  $\text{AlF}^+$ , was compared to that of a  $\text{K}^+$  beam, which serves as a reference. By means of the TOF spectra after the trap, the breakup of the bi-atomic beams was observed.

The spectra confirmed previous findings, that  $\text{CO}^+$  partly breaks up such that several beam components exit the trap. In the  $\text{AlF}^+$  breakup, on the contrary, neither  $\text{F}^+$  nor  $\text{AlF}^+$  ions are observed, but the beam after the trap is composed of  $\text{Al}^+$  only. For the loss rate measurement, the storage time of the ions in REXTRAP was systematically changed. A beam gate enabled a gated injection into the trap, such that ions were collected during the first 100 ms of each cycle in the Penning trap (normal trapping potential configuration) and were held until the end of the period time. Thereafter, the ions were extracted in the normal way and sent to the EBIS for charge breeding. Table 3 summarizes the ion types tested and measured.

Beam into trap	Cooling mass	Beam out of trap	Beam after separator
$^9\text{Be}^+$	9	$^9\text{Be}^+$	$^9\text{Be}^{4+}$
$^{13}\text{C}^+$	13	$^{13}\text{C}^+$	$^{13}\text{C}^{6+}$
$^{39}\text{K}^+$	39	$^{39}\text{K}^+$	$^{39}\text{K}^{10+}$
$^{27}\text{Al}^{19}\text{F}^+$	27	$^{27}\text{Al}^+$	$^{27}\text{Al}^{7+}$
$^{13}\text{C}^{16}\text{O}^+$	13	$^{13}\text{C}^+$ ( $^{16}\text{O}^+$ ), $\text{H}_2\text{O}^+$ and $^{13}\text{C}^{16}\text{O}^+$	$^{13}\text{C}^{4+/6+}$

Table 3. Overview of beams and cooling parameters during the holding-time measurement. Beam compositions are given before and after REXTRAP, as well as the beam selected by the REX separator. While the CO beam break up in multiple components in the trap, the AlF beam breaks up fully only leaving Al after the trap and all F is removed.

Figure 8 shows the intensity after the EBIS and separator, as a function of the period time. Measurements with  $\text{K}^+$  and  $\text{CO}^+$  were taken over a wide intensity range ( $10^7$  -  $10^9$  particles injected per pulse into the Penning trap), which had no systematic effect on the loss rate. For the representation in Figure 8, the intensities in each measurement series have been normalized to the first measurement point at 100 ms, which corresponds to no additional holding time after the collection of ions into the trap has stopped. Potassium is relatively unaffected by long holding times: when cooling on  $A=39$ , the  $\text{K}^+$  ions can be stored in the trap for up to 900 ms period time without measurable losses. Uncooled,

the population in the Penning trap decays with a half-life in the order of 50 ms. The  $\text{AlF}^+$  beam, which breaks up such that only  $\text{Al}^+$  remains in the trap, shows an almost identical behaviour. Furthermore, it should be stated that  $\text{Xe}^+$  can also be kept in REXTRAP for more than a second, which was demonstrated during an earlier experimental campaign [33].

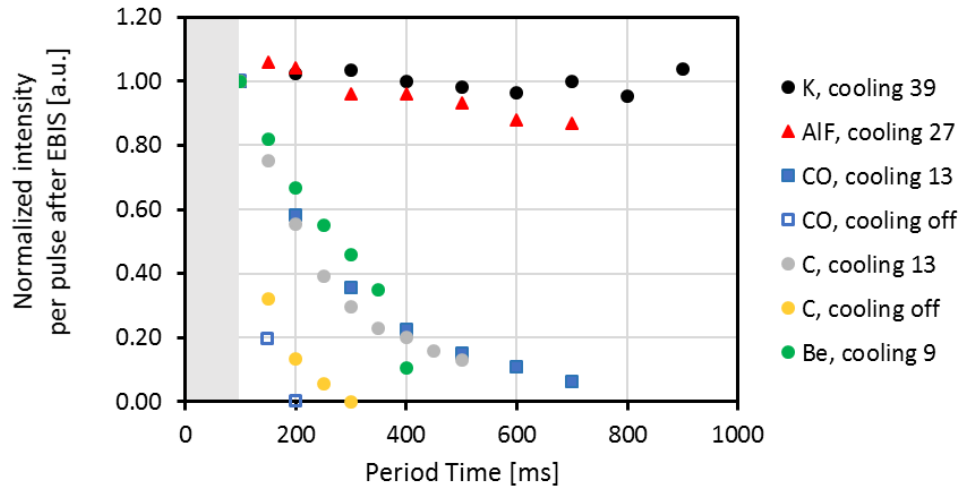


Figure 8. Ion loss measurement with the beam gate open during the first 100 ms of each cycle, indicated by the grey bar. While the output per pulse from the charge breeder of K and Al does not change significantly with longer holding times in the Penning trap, the carbon and beryllium beams decrease rapidly.

$\text{CO}^+$ , when cooling on carbon, however, behaves differently: losses are experienced when attempting to store the ion cloud in the trap for longer times. The  $\text{CO}^+$  beam is lost exponentially with a half-life of around 100 ms. When  $\text{CO}^+$  is not cooled, the ion losses are significantly higher than in the case of the uncooled K beam. Almost identical loss rates for  $\text{C}^+$  and  $\text{CO}^+$  beams were found, which is expected if one assumes the  $\text{CO}^+$  molecule breaks up upon injection into the trap. The holding time for  $\text{Be}^+$  is similar to that of  $\text{C}^+$ .

The mechanism behind the losses could not be fully explained within this study. If it would be due to charge exchange, one would see a progressive increase of another ion species in time (see e.g. [33]), which is not the case. The ionisation potential of carbon (11.3 eV) is similar to that of xenon (12.1 eV) and can therefore not explain the difference either. If the losses would be due to the mass effect hampering the trapping of light ions, one would expect to see an even worse holding time for  $^9\text{Be}^+$  than for  $^{13}\text{C}^+$ , which is not the case. Possibly impurities in the vacuum system cause unwanted chemical reactions between the carbon and for example  $\text{H}_2\text{O}$ .

### 3.2 Pulsed injection into the EBIS

At the start of this study, pulsed injection into the EBIS with prior cooling and bunching in a Penning trap had been proposed as charge breeding scheme for a synchrotron-based  $^{11}\text{C}$  therapy facility [3]. Within the investigations presented in this work, however, we have found that its working range is strongly limited, which makes it unsuitable for a therapy purpose. Nevertheless, the scheme serves as an important reference case as it represents the normal operating scheme of the charge breeder system.

In this section, the efficiency of the charge breeding stage and breakup characteristics of two different injection schemes into REXTRAP are compared: the normal and the flat trap configuration. Above, we have shown that the breakup of the  $\text{CO}^+$  molecules inside the Penning trap can partly be avoided by lowering the injection energy into the trapping region. In the normal trap configuration most of the molecules break up, hence, the beam is cooled on  $A=13$  as atomic carbon ions make up the largest

part of the beam extracted from REXTRAP. In the flat trap configuration, the injection energy is lower in order to reduce the breakup upon injection into the buffer gas, therefore the beam is cooled on A=29 and mostly CO<sup>+</sup> molecules are extracted from REXTRAP.

As previously mentioned, only the beam species that have been sufficiently cooled can be injected into the EBIS efficiently. Thus, in order to correctly compare the efficiency of the beam preparation inside the Penning trap for the two trap configurations, the beam has to be taken through the EBIS. The transmission of carbon through the whole charge breeder stage was measured for relatively low CO<sup>+</sup> beam intensities, i.e. <100 pA. In this case the beam was not gated, but the ions were constantly injected into the Penning trap throughout the period time, as would be the case for a treatment facility. Thereafter the cooled ion bunch was transmitted to the EBIS for charge breeding in the normal way.

The black curves in Figure 9 represent the trap transmission. The normal trap has a higher transmission than the flat trap, due to better injection conditions, and faster cooling during the first axial oscillation. In both cases, the trap transmission decreases with longer period times due to two effects. First, for longer holding times in REXTRAP the ions suffer more from the high loss rate discussed above. Second, space charge effects in REXTRAP become more relevant, as the injection is continuous and higher integrated intensities need to be accumulated during longer period times (e.g. 2.8·10<sup>8</sup> charges are injected for a 500 ms period time). When the accumulated charge per pulse approaches, and exceeds, the space charge limit of the Penning trap (see Sec. 3.3.2 below), the efficiency decreases.

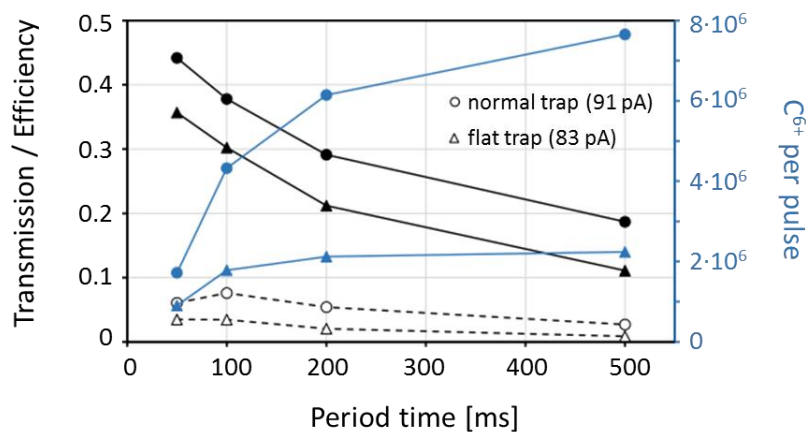


Figure 9. Transmission through REXTRAP (black solid line, including exiting C<sup>+</sup>, O<sup>+</sup>, H<sub>2</sub>O<sup>+</sup> and CO<sup>+</sup> beams) and total efficiency of carbon ions (charge bred to C<sup>6+</sup>) through REXTRAP and REXEBIS (dashed) for a normal (circle) and a flat (triangle) axial trapping potential in the Penning trap, with an input beam of 91 pA and 83 pA, respectively. The blue curves correspond to the total number of C<sup>6+</sup> ions extracted from the charge breeder system.

The over-all efficiency (dashed curves in Figure 9) of the charge breeder system for C<sup>6+</sup>, including REXTRAP and REXEBIS, has an optimum around 100 ms period time and is higher for the normal than for the flat trap configuration. For shorter period times, the breeding time in the EBIS is insufficient, while for longer period times losses and space charge effects in REXTRAP become important and reduce the efficiency. With the normal trap configuration at 100 ms period time, a maximum total efficiency of 8% through REXTRAP and REXEBIS could be achieved, corresponding to 4.3·10<sup>6</sup> extracted C<sup>6+</sup> ions per bunch when injecting 91 pA of CO<sup>+</sup> beam into the charge breeder system, i.e. into REXTRAP. For longer period times, higher particle numbers up to 7.7·10<sup>6</sup> C<sup>6+</sup> ions per pulse could be extracted with a trade-off in efficiency. The measurements showed similar efficiencies and particle numbers for charge states 4<sup>+</sup>, 5<sup>+</sup> and 6<sup>+</sup>, when optimizing the breeding time in the EBIS. For the lower

charge states, the optimum in efficiency is reached at a shorter period time, as a shorter breeding time is sufficient.

In conclusion, the attempt to keep the molecules intact through REXTRAP using a flat trapping potential can be discarded due to the lower over-all efficiency compared to the normal trap configuration. Furthermore, even if the normal trap configuration has a reasonable maximum efficiency of 8% for the charge breeder system, when going to long period times it decreases significantly. The efficiency decreases even further for higher beam intensities, which is addressed in the next section. Therefore, standard operation charge breeding of  $\text{CO}^+$  together with a low-repetition-rate synchrotron would be highly inefficient.

### 3.3 Space charge limitations of REXTRAP and REXEBIS

Under normal conditions at ISOLDE, space charge does not play a role as typical ion currents are small compared to the capacity of the devices. As this is not true any longer for the  $\text{CO}^+$  charge breeding system, where significant currents need to be handled, we have made efforts to determine the intensity limitations in REXTRAP and REXEBIS. Even though the theoretical space charge limits can be calculated as described in Sec. 2.2.3 and Sec. 2.3, the practical ion holding capacity might differ. In the trap, for example, the actual cloud size and compression are unknown and in the EBIS the neutralization factor  $k$  (Eq. 2) might change with different experimental conditions, such as the mode and tuning of the injection.

In order to quantify the effect, we have conducted dedicated test measurements to experimentally determine the holding capacity of REXEBIS and REXTRAP. They will help to understand which of the devices is the bottleneck and therefore causes the losses seen in Figure 9.

#### 3.3.1 Space charge limitations in REXEBIS

In order to establish a limit for the EBIS space charge neutralization, the current saturation was measured after the EBIS without prior cooling of the beam in the Penning trap, to exclude a possible current limitation from the trap. To mimic the timing of a pulsed injection into REXEBIS, without actually bunching the beam in REXTRAP, a fast solid-state switch (50 ns switching time) was connected to an electrostatic deflector before the Penning trap. Thereby, the continuous beam from GPS was chopped into pulses of 60  $\mu\text{s}$  length at 10 Hz. The beam was transmitted through the Penning trap without trapping, as neither an axial trapping potential (see 'continuous' trap configuration in Figure 4), nor buffer gas or RF cooling were applied. Since most of the beam was discarded by the chopper, high particle currents from the  $1^+$  ion source were required. The available  $\text{CO}^+$  intensities were not sufficient for this test, therefore we measured the space charge saturation with an argon beam, which could be produced abundantly by injecting argon gas into a VADIS target ion source. For example, a  $^{40}\text{Ar}^+$  current of 14.8  $\mu\text{A}$  from GPS translated into approximately  $1.1 \cdot 10^9$  ions per pulse being injected into REXEBIS, taking into account the 80% transmission losses (mainly occurring in the GPS).

Figure 10 shows the Ar beam (black), measured after the REX separator for an increasing number of particles injected into REXEBIS. The  $\text{Ar}^+$  current was varied by changing the argon gas pressure at the GPS ion source, and the optimal breeding time varied between 40 and 45 ms. The EBIS neutralization value  $k$  (blue) was calculated as the ratio of total number of charges extracted per pulse from the EBIS (including all Ar charge states, as well as other residual gas ions produced in the electron beam, measured before the mass separation in the REX separator) and the total space charge capacity of the device ( $2.3 \cdot 10^{10}$  charges). Here, we neglect that the extraction efficiency might be slightly  $<100\%$ . At approximately  $7.5 \cdot 10^8$  injected charges, space charge effects in the EBIS start becoming visible and cause a saturation of the total extracted current and thereby of the filling  $k$ . The measured  $k$  value of the EBIS at this point was 25%. For higher injected currents, a  $k$ -value of 30% could be achieved. The

$^{40}\text{Ar}^{11+}$  current actually saturates a bit earlier than the total extracted current, as the CSD may peak at lower charge states due to the less deep potential depth of the highly compensated electron beam. The less deep potential well reduces the ability to keep highly charged ions, that are hotter than the cool low-charged ions. In Table 4, the number of ions in a certain charge state is calculated according to Eq. 3. As no Ne buffer gas was injected into the Penning trap during the measurement, the background from residual gas ions was as low as  $10^8$  charges per pulse, corresponding to a filling of 0.4% of the electron beam. At low neutralization,  $\sim 20\%$  of all Ar ions in the EBIS are expected to be in charge state  $11^+$  at optimal breeding time. However, for a high neutralization of 25%, the fraction in charge state  $11^+$  may be lower. As only  $8.5 \cdot 10^7$   $^{40}\text{Ar}^{11+}$  are extracted from the EBIS, one can conclude that the fraction of Ar in charge state  $11^+$  has been reduced to approximately 17% ( $f=0.17$  in Table 4).

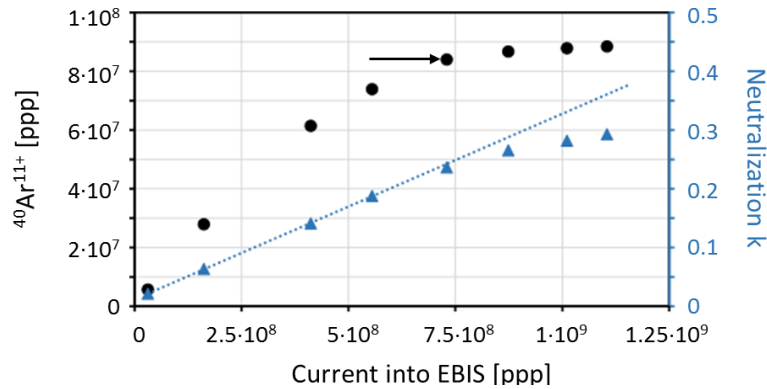


Figure 10.  $^{40}\text{Ar}^{11+}$  intensity after the REX separator in particles per pulse (black) and neutralization  $k$  of the EBIS (blue), for an increasing  $^{40}\text{Ar}^+$  input intensity. Above  $7.5 \cdot 10^8$  particles injected into the EBIS, saturation effects start to become visible, as indicated by the black arrow. The total  $^{40}\text{Ar}^{11+}$  output saturates at  $9 \cdot 10^7$  ions per pulse. A neutralization of 30% could be obtained.

Finally, the findings from the Ar measurements have to be translated to a  $\text{CO}^+$  case. Let us assume that the neutralization is comparable to that of Ar, when injecting  $7.5 \cdot 10^8$  charges of  $\text{CO}^+$  beam from REXTRAP, namely  $k=25\%$ . This is a reasonable approach even though the actual  $k$  value might vary slightly due to different ion injection tuning, as well as with different nuclear charge  $Z$  of the injected ions. If we then repeat the calculation for the  $\text{CO}^+$  case (see Table 4), assuming that 50% of the beam extracted from the EBIS is made up of carbon and that the rest of the electron space charge potential is filled mainly with oxygen and a small fraction of residual gas ions, Eq. 3 gives an expected output of  $2.1 \cdot 10^8$   $^{13}\text{C}^{6+}$  ions per pulse at 25% neutralization. This particle number describes a conservative situation where  $\text{CO}^+$  is injected into the EBIS and oxygen fills approximately half of the EBIS space charge potential. However, when cooling in REXTRAP beforehand, the molecules break up and when cooling on  $A=13$ , mostly carbon will be injected into the EBIS, meaning that  $\delta$  might well be  $>0.5$ . In addition, the reduction in phase space for cooled ions leaving the Penning trap, which was not the situation for the chopped  $\text{Ar}^+$  beam, may also yield a higher  $k$  value.

Beam	$^{40}\text{Ar}^{11+}$	$^{13}\text{C}^{6+}$
$k$	0.25	0.25
$\delta$	0.99	0.5
$f$	0.17	0.4
$\langle Q \rangle$	11	5.5
<b>Ions after separation [ppp]</b>	<b><math>8.6 \cdot 10^7</math></b>	<b><math>2.1 \cdot 10^8</math></b>

Table 4. Number of  $^{40}\text{Ar}^{11+}$  and  $^{13}\text{C}^{6+}$  ions that is possible to extract from REXEBIS according to Eq. 3 for realistic charge state distributions of Ar and CO beams for a space charge filling of 25%.  $\langle Q \rangle$  is the average charge state over all elements.  $\delta$  and  $f$  are the beam fractions occupied by the corresponding element and charge state, respectively. A background of  $k=0.004$  or  $10^8$  charges from residual gas ions is assumed.



### 3.3.2 Space charge limitations in REXTRAP

In the next step, the practical space charge limit in REXTRAP was determined with a  $\text{CO}^+$  beam. As the trap transmission does not provide sufficient information about the trap cooling efficiency, one has to take the extracted beam also through the EBIS and the REX separator. Thereby, beam components that are transmitted through the trap but lie outside the EBIS acceptance are discarded and the measurement is representative of the space charge limit for beam that was actually cooled in the trap. For this measurement, the  $^{13}\text{CO}^+$  beam was taken from GPS through the charge breeder operating in normal mode, bunching in REXTRAP at a repetition rate of 10 Hz, with the REX separator set to  $^{13}\text{C}^{6+}$ . As shown above, most of the molecules break up upon entering the Penning trap, hence, the RF cooling frequency was tuned for mass 13.

Figure 11 presents the transmission through REXTRAP, the combined transmission of BTS, REXEBIS and the REX separator and the total transmission through the charge breeder system. All of them decrease for an increasing input current, the trap transmission from initially 38% ( $6 \cdot 10^7$   $^{13}\text{C}^+$  injected) to only 13% when injecting  $4 \cdot 10^9$   $^{13}\text{CO}^+$  ions per cycle.

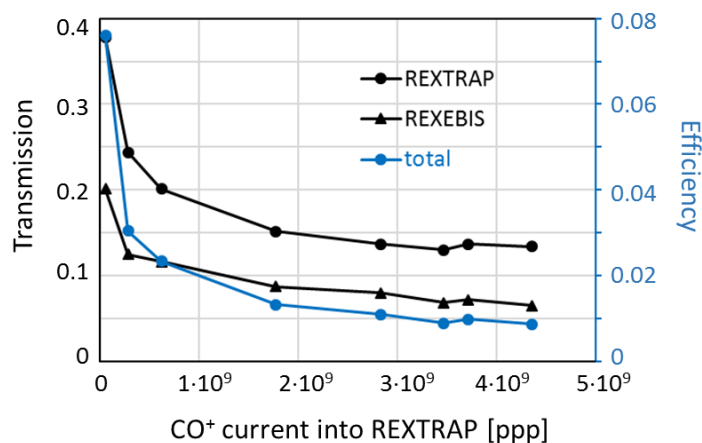


Figure 11. Current dependent transmission through the Penning trap, from the trap exit through the EBIS (including BTS (beam transfer section) and separator); and total efficiency from the Penning trap entrance to after the REX separator.

The plot in Figure 12 shows the same data in a different way. The beam intensity after REXTRAP (black) and after mass selection (blue) saturate for an increasing input current into the Penning trap. Figure 12 is actually non-linear throughout the full measurement range, meaning that saturation effects are present latest at  $7 \cdot 10^7$  charges extracted from REXTRAP, corresponding to the second measurement point in the data series.

At the data point for the highest injected current, indicated by the black arrow, approximately  $6 \cdot 10^8$   $^{13}\text{C}^+$  ions were extracted per pulse from REXTRAP and further transported to the EBIS. Above, we have shown that saturation effects in REXEBIS in pulsed mode start to appear at a filling of 25% corresponding to at least  $2.1 \cdot 10^8$   $^{13}\text{C}^{6+}$  ions after the separator. The measurements presented in Figure 12, however, show that only  $4 \cdot 10^7$   $^{13}\text{C}^{6+}$  ions per pulse (blue data point) could be extracted. This confirms the previous conclusion, that REXTRAP is in space charge saturation, as the measured intensity after the EBIS is a factor 5 lower than what would be expected for a properly cooled input beam.

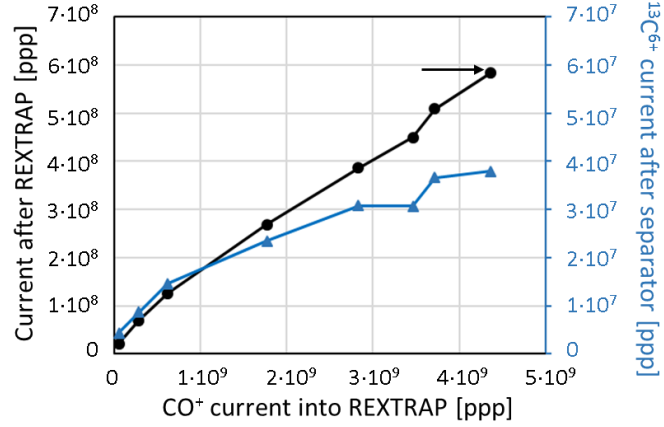


Figure 12. Total beam intensity after REXTRAP (black) and  $^{13}\text{C}^{6+}$  intensity after the separator (blue) in particles per pulse for an increasing  $^{13}\text{CO}^+$  input intensity. The total  $^{13}\text{C}^{6+}$  output saturates at around  $4 \cdot 10^7$  ions per pulse.

We conclude that the EBIS capacity was indeed not limiting the throughput, rather was the beam not completely cooled due to space charge effects in REXTRAP, thereby reducing the injection efficiency into REXEBIS. Table 5 shows where saturation effects due to space charge limitations start to become important in REXTRAP and REXEBIS. In the REX-ISOLDE case, the Penning trap turns out to be the bottleneck. A stronger solenoidal field of the Penning trap could increase its capacity, possibly with a factor 4 going from the present 3 T to a 6 T field (c.f. Eq. 5). Furthermore, one has to implement a correctly working rotating wall cooling scheme, in order to reach the maximum compression of the ion cloud and approach the Brillouin limit, which is currently not the case at REXTRAP where sideband cooling is the dominating effect. State-of-the-art EBISes can have a factor 10 higher space charge capacity than REXEBIS, so there would potentially be room for improvements. The measured values can in principle be pushed towards the theoretical limits, given by Eqs. 1, 3 and 4, at the cost of efficiency. However, as the number of  $^{11}\text{CO}$  from the production stage is limited, a significant reduction in efficiency is not acceptable. In a charge breeder setup based on this concept, aiming for  $^{11}\text{CO}^+$ -to- $^{11}\text{C}^{6+}$  transformation and subsequent injection into a low-repetition-rate synchrotron, the high number of ions collected over the long period time, would make the process very inefficient.

Device	Extracted charges
REXTRAP	$< 7 \cdot 10^7$
REXEBIS	$5.8 \cdot 10^9$

Table 5. Number of charges extracted from REXTRAP and REXEBIS, respectively, where space charge effects are observed for ions in the mass region of interest. The value given for the EBIS corresponds to a filling of 25%. Higher  $k$  values can indeed be obtained, but at the cost of efficiency.

### 3.4 Continuous injection into the EBIS

When repetition rates below 1 Hz are required, a setup with a Penning trap (Figure 13, top) is not advantageous due to the high loss rate for CO and the limited space charge capacity, as discussed above. Therefore, continuous ion injection into the EBIS without prior cooling and bunching in REXTRAP was tested [34]. For this operational mode of the EBIS, the outer barrier of the axial trapping potential - which is usually low during the injection and high during breeding - is constantly at an intermediate voltage. Ions are injected with a certain residual energy above the barrier. During the injection, a good overlap of the ions with the electron beam is essential. If the ions are not injected fully into the electron beam, they will perform oscillations around the electrons and spend only a fraction of their time inside the beam. In the worst case, they circle the electron beam with no overlap. As the outer barrier is never completely closed, ions will escape over the barrier, unless they are

ionized from  $1^+$  to  $2^+$  or a higher charge state by the electron beam during their first round-trip along the EBIS axial trapping potential. As this injection mechanism is in general less effective compared to the pulsed injection [35], where the ion bunch is trapped axially through the outer electrostatic barrier, a reduced trapping efficiency in the electron beam is expected. In the continuous injection mode the loss rate from boil-off of hot ions is higher compared to pulsed injection, as the energy distribution is shifted towards higher energies due to the injection conditions. In addition, the low barrier facilitates axial losses.

For the measurements presented in this section, the beam was transmitted through REXTRAP without cooling (i.e. ‘continuous’ trap configuration), analogously to the operation with the Ar beam described in the previous section. The  $\text{CO}^+$  beam was injected continuously over the barrier into REXEBIS during the full period time, as schematically shown in Figure 13, bottom. For long period times,  $6^+$  is certainly the most dominant charge state being extracted from the EBIS, as the charge breeding process continues during the full period time and lower charge states are over-bred.

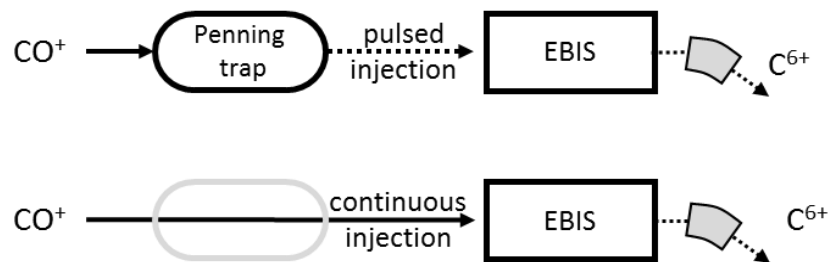


Figure 13. Schematic drawing of REX low-energy stage in pulsed (top) and continuous (bottom) injection mode.

The efficiency of charge breeding to  $\text{C}^{6+}$ , including injection into REXEBIS, breeding and separation, is shown in Figure 14 for beams of two different intensities as a function of period time. Due to space charge limitations in the EBIS, efficiencies for the higher injected intensity of 3.6 nA are significantly lower. For both intensities, the total number of extracted ions (blue) increases for longer period times, as more ions are collected per cycle. At the same time, as more charges are accumulated, space-charge related losses become more pronounced. There is an optimum in the efficiency around 200 ms period time. For shorter period times, the breeding into charge state  $6^+$  is inefficient, as the lower charge states still dominate. The observed decrease in efficiency for long period times is a combined effect of ion boil-off and space charge limitations in the EBIS. In order to disentangle the two effects, we have studied them independently.

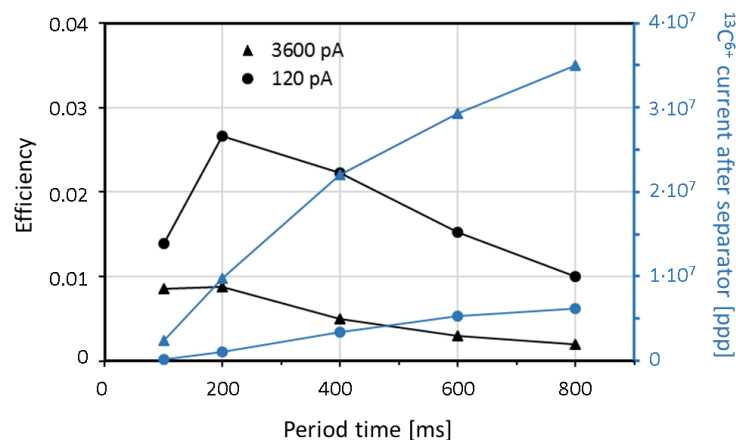


Figure 14. Efficiency (black) and numbers of extracted  $^{13}\text{C}^{6+}$  particles (blue) as function of the period time in continuous injection mode for two injection currents: 3600 pA (triangles) and 120 pA (circles).

To determine the boil-off in the EBIS without introducing space charge related problems, beam was injected during 90.5 ms and then stored in the EBIS for various period times. Figure 15 shows how the charge breeding efficiency to  $C^{6+}$  changes with the holding time and for different input intensities. Overall, the efficiency for the higher injected current is lower due to space charge limitations in the EBIS. However, as always the same number of ions is injected at the beginning of each cycle, space charge related effects do not influence the behaviour within one measurement series. For longer holding times, we suffer from a boil-off of ions in the EBIS, however, we cannot distinguish between radial and axial losses. The number of extracted ions per pulse peaks at 200 ms breeding time as the breeding to charge state  $6^+$  continues after the injection window. The required breeding time to reach the highest charge state is longer than the optimal breeding time of 70 ms for pulsed injection. The extended breeding time can be explained by a poor radial overlap of the ions with the electron beam, i.e. a low effective electron current density, that is a consequence of the continuous ion injection.

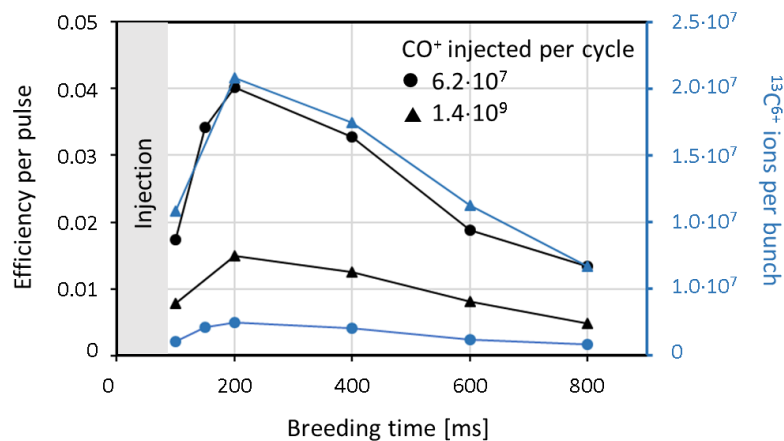


Figure 15. EBIS efficiency into charge state  $^{13}C^{6+}$  (black) and particle current after separator (blue) for an injected current of  $6.2 \cdot 10^7$  (circles) and  $1.4 \cdot 10^9$  (triangles)  $CO^+$  molecules. Beam is injected continuously into the EBIS during the first 90.5 ms of the period time (grey region) and further charge bred until the end of the cycle.

Figure 16 quantifies the decrease of efficiency coming from the limited space charge capacity of the EBIS. Here, the period time is constant within one measurement series, but the current input that is injected continuously, increases. For 100 ms period time, the current is already saturated at a few  $10^7$   $C^{6+}$  ions extracted from the EBIS. This exemplary case corresponds to only 1% neutralization of the electron beam. It seems, that in the continuous injection mode, we cannot fill the EBIS properly as we do in the pulsed injection mode with a beam pulse length  $< 30 \mu s$ . In addition, the  $1^+$  to  $6^+$  breeding efficiency in the order of 1% is extremely poor.

The low filling grade can be explained through a combination of poor injection efficiency and high loss rates through boil-off of hot ions. As we have seen above, the breeding time to reach  $6^+$  is longer in the continuous mode, which is a strong indication towards a poor ion-electron overlap and thereby a low trapping probability. In pulsed mode (see Figure 17 left) the outer barrier is low during injection and ions can be injected such that they have a relatively low residual kinetic energy inside the trapping region. When injecting continuously, the barrier is constantly at an intermediate height and  $CO^+$  ions enter the EBIS approximately 125 eV over the barrier (see Figure 17 right). Hence, ions have a higher residual kinetic energy in the trapping region around 240 eV. In the end, an equilibrium between the injected current and all losses is established at a certain  $k$ . For the continuous injection mode the losses upon injection and through boil-off are significant and limit the filling of the EBIS drastically. Operation at RHIC EBIS has shown that a higher neutralization during continuous injection can be achieved when orders of magnitudes higher currents are injected, hence, at the cost of efficiency [36].

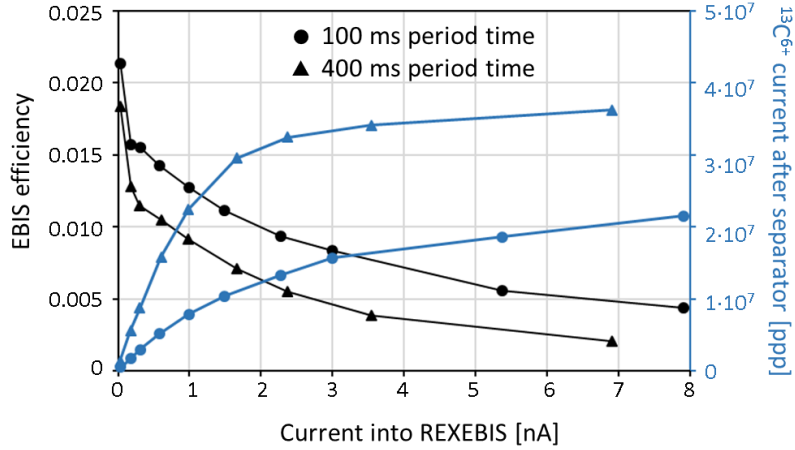


Figure 16. EBIS efficiency into charge state  $^{13}\text{C}^{6+}$  for an increasing input intensity injected continuously during a 100 ms and 400 ms period time.

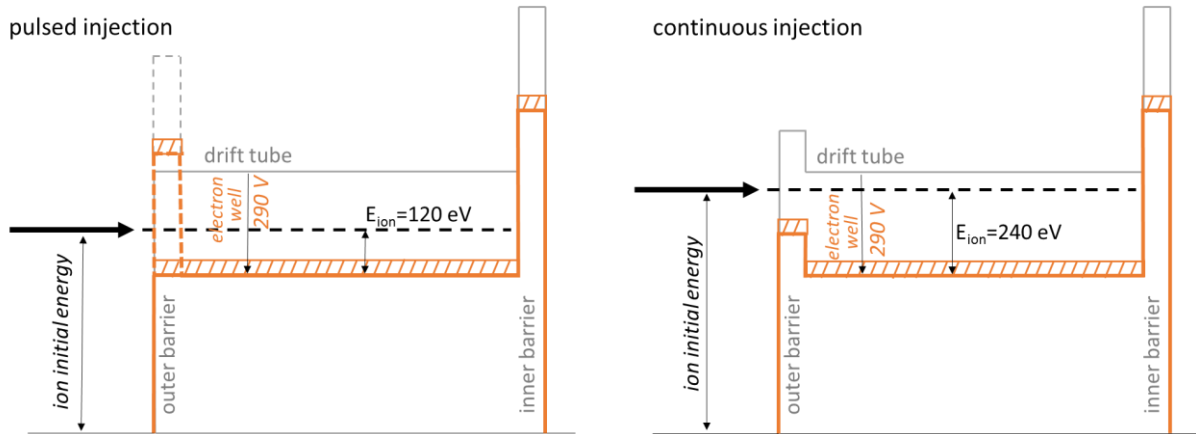


Figure 17. Schematic drawing of potentials for pulsed and continuous injection into the EBIS. The dashed region indicates the radial potential depth of the electron beam, in this case 40 V.

## 4 Challenges in $^{11}\text{C}$ charge breeding

### 4.1 EBIS capacity

In the light of the measurements discussed in the previous chapter, we can calculate the required EBIS capacity to reach the desired intensity output of  $10^{10}$  carbon ions per pulse. In case the subsequent accelerator chain has a high efficiency, this should be sufficient for a single-spill-treatment.

We have learned, that for a pulsed injection into the EBIS with a reasonable efficiency, we can reach a filling of the electron beam of approximately 25% (possibly higher if the beam is cooled before injection). To reach the desired intensity in the pulsed mode, an EBIS with an electron space charge capacity of  $1.2 \cdot 10^{12}$  electrons is required, assuming the same beam filling and CSD as in Table 4. This could be obtained with an EBIS of 10 A electron current, 1.8 m trapping length, and 25 keV electron energy. These specifications are similar to the RHIC EBIS [37] parameters – highly challenging, but in principle within reach with current EBIS technologies. For continuous injection, which is required when the injected pulse length is in the ms instead of  $\mu\text{s}$  range, the filling is significantly lower – in the order of 1%. Thus, for the continuous injection mode, an electron current sufficient to provide  $1 \cdot 10^{10}$  ions is out of technological reach. Figure 18 summarizes the two injection scenarios.

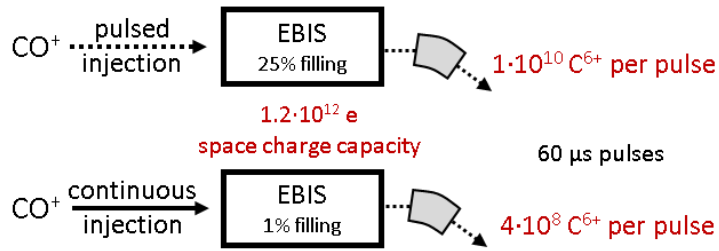


Figure 18. Extracted C<sup>6+</sup> intensity for pulsed and continuous injection into an EBIS, assuming a space charge capacity of 1.2.10<sup>12</sup> charges. The elemental and charge state distribution is taken from Table 4 ( $\delta=0.5, f=0.4, \langle Q \rangle=5.5$ ).

The pulse length of the extracted beam is mainly determined by the trap length and ion energy in the trapping region, as it is limited by the ion's flight time from the trapping region inside the EBIS. It does not depend on the intensity and can be as low as 10 μs, which would translate into an instantaneous current of 4 mA. By applying a ramp of a few 100 V to the drift tubes, the pulse length can be shortened further, however, it is not recommended as 10 μs is sufficiently short and the high instantaneous current would cause significant space charge effects in the low energy transfer line [38]. In addition, the longitudinal energy spread might lead to chromatic aberrations in the extraction and low energy transfer systems. A short pulse length guarantees an efficient multi-turn injection into the synchrotron. Currently, at MedAustron, 50 μs pulses are used for stable carbon beams. The pulse length from the EBIS can be of the same length or shorter, thus ensuring a comparable or even improved efficiency in the multi-turn injection into the synchrotron.

In conclusion, building an EBIS with a capacity that can in principle charge breed 10<sup>10</sup> carbon ions per pulse to charge state 4<sup>+</sup>, 5<sup>+</sup> or 6<sup>+</sup> and extracting them in a sufficiently short pulse, is technically possible. The main challenge is to obtain a reasonable efficiency in the charge breeder system, in particular in the injection into the EBIS.

## 4.2 Efficiency of the charge breeder system

### 4.2.1 Penning Trap + EBIS

The measurements with CO beams at REX-ISOLDE, that were described in the previous chapter, were laid out to investigate the matching of the ISOL-produced CO beam with a medical synchrotron, as proposed by Augusto et al. [3]. There, the authors suggested a charge breeding stage similar to REX-ISOLDE, consisting of an ion trap and an EBIS. Based on previous experience with the charge breeder system, the efficiency was assumed to be 45% in the trap and 30% for the EBIS and separator (see Figure 19).

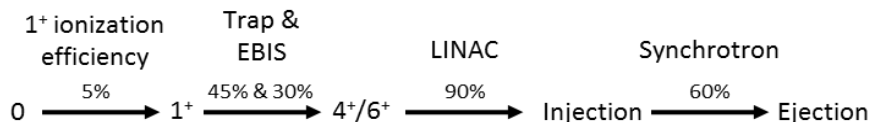


Figure 19. Suggested injection scheme for <sup>11</sup>C from [3].

During our measurement campaigns, however, we have shown that these values are not realistic for a high-intensity charge breeder for hadron therapy due to the high loss rate and the space charge limitations in the Penning trap. Augusto et al. correctly state that 'the limitation comes mostly from the trapping process. When charge breeding CO<sup>+</sup> to C<sup>4+/6+</sup>, the inherent problem is the low repetition rate of the synchrotron and the consequential need of storing the 1<sup>+</sup> ions efficiently. The carbon is lost

in the trap with a half-life of approximately 100 ms, hence, it cannot be used to store the beam during the synchrotron cycles. In addition, the space charge limitation of the trap does not allow for efficient transmission of more than few  $10^8$  ions per pulse, even when increasing the magnetic field from the present 3 T to 6 T.

#### 4.2.2 EBIS only

A beam preparation scheme pursued by Noda et al. [39] refrains from using a Penning trap for storing the  $1^+$  beam, but aims at injecting 10 ms pulses of  $10^{11}$   $^{11}\text{CO}_2^+$  directly into the EBIS. Thereby, an efficiency of the charge breeder and separator of 10% is assumed, and that  $10^{10}$   $^{11}\text{C}^{4+/5+}$  ions are extracted in a 100  $\mu\text{s}$  pulse from the EBIS. With the recent measurement results in mind, the realization of such a scheme seems unrealistic. The pulse length in the ms range of the injected beam requires a continuous injection scheme into the EBIS (in contrast to  $<30$   $\mu\text{s}$  pulses used in pulsed injection). In our tests with REXEBIS, we have found that efficiencies for high-intensity continuous injection are in the sub-percent range, mainly due to a highly inefficient injection and additional losses in the EBIS that prevent an efficient filling of the electron space charge potential. To reach the desired carbon intensity despite the low filling efficiency, an electron beam current significantly higher than the  $1.2 \cdot 10^{12}$  e given in Figure 18, would be required, which is not attainable with state-of-the-art EBIS technologies. In addition, oxygen occupies more of the space charge potential of the EBIS when injecting a dioxide rather than the monoxide.

#### 4.2.3 RFQ cooler + EBIS

An improvement of the  $\text{CO}^+$  to  $\text{C}^{4+/6+}$  charge breeding scenario is the use of an RFQ ion beam cooler for cooling and bunching [40] before injection into the EBIS instead of a Penning trap. The RFQ cooler is a linear Paul trap filled with a buffer gas. An RF voltage is applied to the quadrupole rods, which confines the particles radially. The particles follow a stable trajectory if the Mathieu parameter  $q_{\text{Mathieu}}$  is limited:

$$q_{\text{Mathieu}} = \frac{4qV_{\text{RF}}}{mr_0^2\omega_{\text{RF}}^2} < 0.908 \quad (7)$$

with the particle charge  $q$ , the zero-to-peak voltage  $V_{\text{RF}}$ , the ion mass  $m$ , the radius of the circle inscribed to the RF rods  $r_0$  and the RF frequency  $f_{\text{RF}} = \omega_{\text{RF}}/2\pi$ . Thereby, the depth of the radial trapping potential is linear with the voltage, meaning that a high voltage is required in order to have a large capacity. If no DC component is applied to the RF rods, the cooler acts as high-pass mass filter, and therefore all components,  $\text{C}^+$ ,  $\text{O}^+$  and  $\text{CO}^+$ , can be cooled at the same time.

Within the framework of MEDICIS-Promed, tests with  $\text{CO}^+$  inside the ISOLDE RFQ-cooler ISCOOL have been performed. The goal, however, was not to study the efficiencies for bunched, high-intensity operation, but to evaluate the breakup of  $\text{CO}^+$  molecules under different conditions. Thereby, very little breakup was observed [41], however, the authors have no further data available on the trapping and cooling of high-intensity  $\text{CO}^+$  ion beams in an RFQ cooler. It remains to be demonstrated that no other loss mechanisms are involved under these conditions.

ISCOOL can cool and bunch  $10^8$  charges in one pulse [42], which is similar to REXTRAP. A typical pulse length from a cooler in bunched mode is in the order of several  $\mu\text{s}$  and therefore suitable for injection into the EBIS. In order to overcome space charge limitations and create a deeper radial trapping potential, a more powerful RF setup is required. SHIRaC is a buffer-gas filled RFQ cooler at GANIL, optimized for high-intensity radioactive beams and typically used in continuous mode [43]. There, up to 9 kV and 9 MHz - compared to several 100 V RF amplitude at ISCOOL - can be applied to the RF rods, enabling the transmission of  $\mu\text{A}$  of continuous beam. The voltage is limited by electrical breakdowns, as the rods have to hold the voltage in a gas-filled environment. The ratio of the demonstrated 9 keV/9

MHz are ideal for transmission of their test beam  $^{133}\text{Cs}^+$ . With amplitudes  $>1$  kV as has been demonstrated in the SHIRaC at LPC-Caen, the space charge limit can probably be stretched to  $10^9$  possibly even to  $10^{10}$  charges. According to Eq. 7, a higher frequency of at least 22 MHz would be required for transmission of the significantly lighter  $^{11}\text{C}^+$  at the same high voltage, which is highly challenging for the RF setup.

Furthermore, the effect of the high ion number on the transverse emittance is crucial. In [44] Boussaid et al. show that the emittance increases proportionally to the beam current. The transverse normalized emittance for a  $^{133}\text{Cs}^+$  beam grows from 0.001 to 0.0025 mm mrad, 4-rms, when increasing the continuously extracted current from 100 nA to 1  $\mu\text{A}$ . If  $1 \cdot 10^{10}$  particles are to be extracted within 20  $\mu\text{s}$ , that corresponds to a current of 80  $\mu\text{A}$ , and the transverse emittance might therefore be high (a plain linear extrapolation suggests 0.125 mm mrad, 4-rms). This is larger than the acceptance given by Eq. 4, using RHIC-EBIS parameters for a Cs beam, thus a poor injection efficiency into the EBIS is expected.

In conclusion, operation with an RFQ ion beam cooler as a buncher before the EBIS is limited in intensity. The capacity of the cooler may be pushed towards  $10^9$  to  $10^{10}$  particles, although with a large transverse emittance, resulting in a maximum of  $10^9$   $^{11}\text{C}^{6+}$  per bunch after an EBIS. However, the high intensity is challenging for the RFQ design due to the low mass of the carbon ions that requires higher frequencies than are available at state-of-the-art devices. In addition, no data on potential other loss mechanisms is presently available to the authors. The desired intensity of  $10^{10}$  carbon ions out of the EBIS seems out of reach with this method, which is therefore only suitable if the intensity requirements can be relaxed.

## 5 Alternatives to $\text{CO}^+$ injection

Alternatively to storing  $1^+$  ions and injecting them into the EBIS, one may want to consider storing the produced radioactive isotopes as neutral molecules and release them directly into the EBIS in gaseous form. A setup based on a similar concept, although with an ECR ion source, is described in [45]. An advantage of neutral gas injection is that higher  $k$  values, up to  $>0.7$ , can be obtained for the EBIS. In this case, it is sufficient if the release time of the neutral molecules is in the order of some 10 ms, as the EBIS has an inherent storing capability for this time. A cryogenic trap in the vicinity of the electron beam, preferably inside the EBIS, is suggested. The neutral molecules would freeze on a cold surface (melting point  $\text{CO}$ : 68.13 K [46],  $\text{CH}_4$ : 90.58 K [46]) and be released into the electron beam by heating of the trap. Boytsov et al. [47] have successfully demonstrated the storing of  $\text{CH}_4$  in such a cryogenic trap, cooled with liquid He, as well as the neutral gas injection into the electron beam of their ESIS (Electron String Ion Source) through a heating pulse of 2 ms. The conversion efficiency from frozen  $\text{CH}_4 \rightarrow \text{C}^{4+}$  of 5-10%, obtained in tests with stable  $^{12}\text{CH}_4$ , is indeed very promising.

Coupling the cryogenic trap to an ECR ion source instead is not a valid alternative, as the ECR ion source does not have a storing capability, when operated in normal mode. The pulse length out of the source would be determined by the release time of the cryogenic trap convoluted by the effusion time to the ECR plasma and the ionisation time to reach the desired charge state, which is orders of magnitudes longer than the pulse length desired for injection into the accelerator. Afterglow operation [48] provides a certain degree of storage for heavier ions, although it would need to be proven for light carbon. Furthermore, the extracted pulse length from an ECR ion source in afterglow mode is in the order of few ms and therefore too long for injection into the subsequent accelerator.

If the output from the target (gas or solid) is injected directly into the EBIS (see Figure 20), losses in the gas transport from the target to the cryogenic trap can be minimized by keeping transport



distances as short as possible. A few meters are realistic, considering that the target area needs to be shielded. The sticking of CO to stainless steel has been found to be negligible (sojourn time  $1 \cdot 10^{-11}$  s) [49], which would result in an efficient transport. A possible complication is, that contaminations from other elements and from radiogenic  $^{12}\text{C}$  compounds that effuse from the target to the EBIS may occupy a significant fraction of the electron space charge potential. The target development within the MEDICIS-Promed network is ongoing [50] but no data is so far available to the authors, regarding contaminations. A separation of some sort is most probably required, to obtain a reasonable purity of the gas in the cryogenic trap. An approach to separate the desired gas component from contaminations is a gas separation system, as, for example, the cryogenic separation system developed by Katagiri et al. [51]. However, it might be challenging to reach the desired purity and efficiency with such a system. Alternatively, a  $1^+$  ion source and mass selection in an electromagnetic spectrometer, as it is done in the usual ISOL-scheme, can be considered, with a subsequent transfer and collection of the gas molecules in the cryogenic trap.

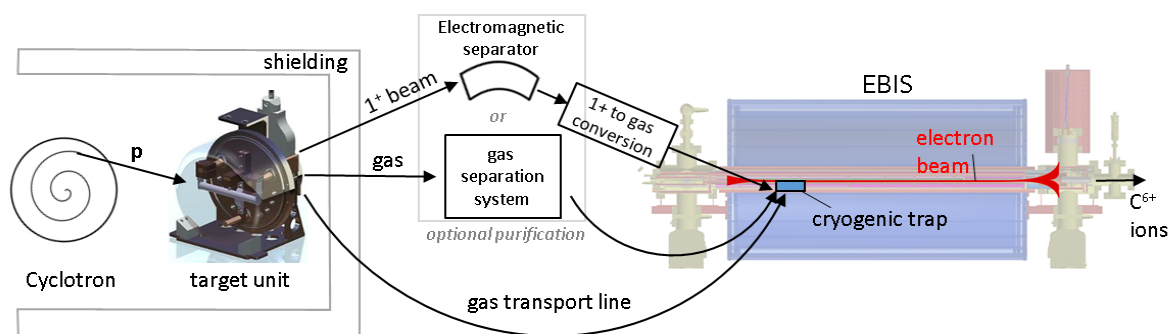


Figure 20. Gas injection into the EBIS, equipped with a cryogenic trap. The radioisotopes are produced from a cyclotron-produced proton beam on a target in a shielded area. The radioactive gas ( $\text{CO}$  or  $\text{CH}_4$ ) is transported into the EBIS, where it is accumulated in a cryogenic trap that releases the molecules through pulsed heating into the electron beam. If the level of contamination of other gases is too high for the EBIS, either a gas separation system or separation of a  $1^+$  beam, in analogy to the ISOL-method, could be applied to purify the target output before injecting into the EBIS.

## 6 Acceleration – green field approach

The largest challenge for the  $^{11}\text{C}$  beam preparation stage discussed above is to provide a high per-pulse-intensity, sufficient to complete a treatment. From a machine point-of-view, one could work with lower currents per spill and make use of more spills. This, however, is not a practicable trade-off, as it extends the treatment time for the patient.

In a state-of-the-art medical synchrotron for carbon ion therapy, only one pulse can be accepted per synchrotron fill. In multi-turn injection, the transverse phase space is completely filled after injection of one pulse, as the phase-space-painting covers the acceptance of the ring. Even if it was not covered immediately after the filling with one pulse, still the injection of multiple pulses from the source would not be possible due to the phase space filamentation in the ring. In a future synchrotron-based therapy accelerator, the accumulation of several pulses in the ring could be realized through electron cooling in the synchrotron [52]. The cooling reduces the transverse emittance in the ring and therefore several pulses can be injected. The method is successfully applied at several storage rings, for example the ESR (Experimental Storage Ring) at GSI [53], ELENA (Extra Low ENERGY Antiproton ring) [54] and LEIR (Low Energy Ion Ring) [55], both at CERN. In a scheme where the patient is treated with several spills from the synchrotron, electron cooling would add considerably to the treatment time, as the cooling time for each pulse might be in the order of 1 s. It would therefore be strictly limited to a single-spill treatment scheme. Assuming that 10 pulses can be accumulated, the intensity requirement on the

EBIS of initially  $10^{10}$  ions would relax to  $10^9$  ions extracted per bunch. However, for a charge breeding system relying on external  $1^+$  ion injection, the extraction of  $10^9$  carbon ions from the EBIS is highly challenging even with a high-power RFQ cooler. Being on the edge of what is technically possible, and taking into account that cooling is not foreseen in any of the existing medical synchrotrons, the method is not recommended for  $^{11}\text{C}$ .

A more natural choice for acceleration of  $^{11}\text{C}$  is a linear accelerator. In comparison to a synchrotron, it can be more easily combined with an EBIS, as both machines are inherently pulsed. Designs of linac-based carbon ion facilities have been proposed by the TERA foundation in the form of CABOTO – Carbon Booster for Therapy in Oncology – an all-linac accelerator for  $\text{C}^{6+}$  ions [56,57], and by CERN within the PIMMS2 study [58]. The repetition rate for the former may be as high as 400 Hz and the beam energy can be changed between pulses by switching on or off the cavities as required. This allows for fast spot scanning of the tumour, which could also follow tumour movement caused by the patient breathing. In substituting the synchrotron with a linac in our  $^{11}\text{C}$  acceleration scheme, one eliminates the two major problems: the high required per-pulse-intensity and the storing of the produced radioactive isotopes, either as molecules or as ions. The primary source concept for stable carbon in the CABOTO design is an EBIS equipped with MEDeGUN [59,60], a high-compression electron gun, developed at CERN. MEDeGUN is designed to provide  $>10^8$   $\text{C}^{6+}$  ions per pulse at 400 Hz from  $^{12}\text{CH}_4$  gas. According to the calculation in [59], which includes gas transport from outside the EBIS to the ionization region,  $9.2 \cdot 10^{-7}$  mbar-l/s or  $3 \cdot 10^{12}$   $\text{CH}_4$  molecules per second need to be provided to the gas supply line in order to reach the desired ion intensity. If this system was to be used for radioactive beam, a gas purification system might be required, as discussed above.

The repetition rate of 400 Hz requires charge breeding to  $6^+$  in under 2.5 ms, which can only be realized in a high-density electron beam. Therefore, the main focus of MEDeGUN is on the high compression of the electron beam, rather than a high capacity. Compared to the RHIC-like EBIS discussed above with an 800  $\mu\text{m}$  electron beam radius, the MEDeGUN beam is highly compressed down to a radius of 60  $\mu\text{m}$ . The small electron beam radius also helps keeping the emittance low, which is beneficial for the design of the consecutive linac. As a drawback, however, the ion injection acceptance is also fairly small: only 0.01 mm mrad for  $^{11}\text{C}^+$  according to Eq. 4 ( $r_{e,\text{trap}} = 60 \mu\text{m}$ ,  $\Delta U_{e,\text{trap}} = 151 \text{ V}$ ), which would complicate a  $1^+$  injection. In our case, however, gas from the target would be injected continuously, thereby completely eliminating the need for storing the produced radioisotopes.

## 7 Summary and Conclusions

Injection into a medical synchrotron requires the EBIS to deliver a pulse of  $10^{10}$  carbon ions within a pulse length of few 10  $\mu\text{s}$ . Ion pulses extracted from an ECR ion source operated in afterglow mode, or by pulsing the introduction of gas into the  $1^+$  ion source with a mechanical valve or through a heating process, have lengths in the ms range. While it is straightforward to achieve a sufficiently short pulse length from an EBIS, the intensity requirement is very demanding. It necessitates an EBIS with high electron beam current, which is, however, within reach of state-of-the-art technology. The challenge is to efficiently store and introduce the radioactive  $^{11}\text{C}$  into the electron beam. Tests have shown that direct, continuous injection of a  $1^+$  ion beam into the EBIS is highly inefficient. For pulsed ion injection, a short pulse length of  $<30 \mu\text{s}$  is required. To reach the short pulse length, a cooler/buncher would be required. The Penning trap and the RFQ ion beam cooler are well-established bunching elements capable of producing short pulses. It was found that the Penning trap cannot store molecular CO beams during synchrotron cycles. No experimental data is available on the transmission and cooling efficiency of high-intensity molecular CO in an RFQ cooler. In any case, both devices have limited space charge capacities that constrain the per-pulse ion output of the charge

breeder. These limits can be overcome by injecting the neutral radioactive gas directly into the EBIS. In order to reach the desired purity of the gas, an intermediate purification step might be required.

Alternatively, different acceleration schemes can be considered, with the goal of reducing the required holding time and per-pulse-intensity from the EBIS, as the classical charge breeding scheme is limited in intensity by the space charge capacity of the cooler/buncher. As an alternative to the synchrotron, the  $^{11}\text{C}$  preparatory stage could be coupled to a linac-based machine, like CABOTO. An electron gun, MEDeGUN, has been specifically designed to be used in an EBIS for  $\text{C}^{6+}$  for CABOTO. The high repetition rate eliminates the need for storing and pulsing the radioactive ions in-between cycles. Instead, a radioactive gas can be injected continuously into the electron beam.

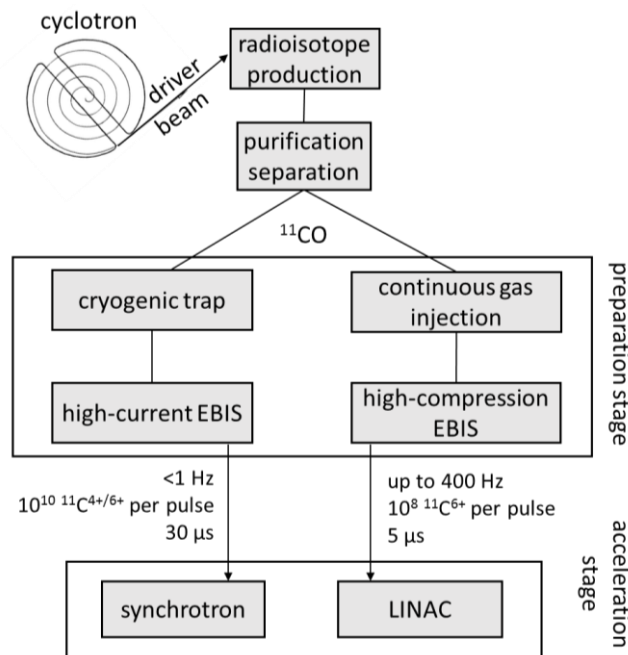


Figure 21. Summary of most promising approaches to  $^{11}\text{C}$  acceleration.

In conclusion:

1. A continuous injection into the EBIS can be excluded due to low efficiency and low output, as the EBIS cannot be filled properly.
2. The Penning trap can be excluded as well due to its low capacity and its inefficiency when storing  $\text{C}^+$  beams.
3. A scheme with an RFQ ion beam cooler and an EBIS is limited to  $10^8$  carbon ions per pulse,  $10^9$  when being optimistic.
4. A promising approach is neutral gas injection via a cryogenic trap into the EBIS. In order not to fill the EBIS with background ion species, the target output could be purified either in a gas separation system or in an electromagnetic spectrometer after  $1^+$  ionization of the target gas, if required.
5. In case of the synchrotron, a high-capacity EBIS with  $1.3 \cdot 10^{12}$  electron charges is required, which is technically possible, but requires significant resources.
6. An EBIS equipped with MEDeGUN, attached to an all-linac accelerator can be more compact than in the case with the synchrotron, as a smaller electron space charge capacity is sufficient and it does not require the cryogenic trap as gas can be injected continuously. Besides the smaller footprint, it possibly also requires lower levels of maintenance and electrical power. The high repetition rate relaxes the per-pulse intensity-requirements, which makes it the most favourable approach.

Figure 21 summarizes the here listed viable scenarios.

## 8 Acknowledgements

This research project has been supported by the European Commission's Horizon 2020 Programme under contract numbers 642889 MEDICIS-PROMED.

This project has received funding from the European Union's Horizon 2020 research and innovation programme under grant agreement No 654002.

## 9 References

1. <https://medicis-promed.web.cern.ch/>
2. T. E. Cocolios et al., 'MEDICIS-Promed: an Innovative Training Network for an new generation in nuclear medicine', IFMBE Proc. vol 65 (2017) 530-533
3. R. Augusto et al., 'New developments of 11C post-accelerated beams for hadron therapy and imaging', Nucl. Instrum. Meth. B 376 (2016) 374-378
4. L. Badano et al., 'Proton-Ion Medical Machine Study (PIMMS)', part 1, CERN-PS-99-010-DI
5. P. J. Bryant et al., 'Proton-Ion Medical Machine Study (PIMMS)', part 2, CERN/PS 2000-007 (DR)
6. S. Rossi, 'The status of CNAO', Eur. Phys. J. Plus, (2011) 126: 78
7. M. Benedikt and A. Wrulich, 'MedAustron – Project overview and status', Eur. Phys. J. Plus (2011) 126: 69
8. H.R. Ravn and B.W. Allardyce, 'On-Line Mass Separators', in Treatise on Heavy-Ion Science, Edt. D. A. Bromley, Plenum Press, New York, 1989, ISBN 0-306-42949-7
9. R. Catherall et al., 'The ISOLDE facility', Journal of Physics G: Nuclear and Particle Physics 44 (9) (2017) 094002
10. T. Mendonca et al., 'Production and release of ISOL beams from molten fluoride salt targets', Nucl. Instrum. Meth. B 329 (2014) 1-5
11. D. Habs et al., 'The REX-ISOLDE project', Hyperfine Interactions 129 (2000) 43–66
12. F. Ames, J. Cederkall, T. Sieber, F. Wenander, 'The REX-ISOLDE Facility: Design and Commissioning Report', CERN-2005-009
13. Y Kadi et al., 'Post-accelerated beams at ISOLDE', J. Phys. G: Nucl. Part. Phys. 44 (2017) 084003
14. P. Schmidt, 'REXTRAP - Ion Accumulation, Cooling and Bunching for REX-ISOLDE', Doctoral thesis, Johannes Gutenberg Universität, Mainz, Germany (2001)
15. F. Ames et al., 'Cooling of radioactive ions with the Penning trap REXTRAP', Nucl. Instrum. Meth. A 538 (2005) 17-32
16. F. Wenander et al., 'REXEBIS - the electron beam ion source for the REX-ISOLDE project', CERN-OPEN-2000-320
17. F. Wenander, 'Charge breeding of radioactive ions with EBIS and EBIT', JINST, 5 (2010) C10004
18. R. Rao et al., 'Beam optics design of the REX-ISOLDE q/m-separator', Nucl. Instrum. Meth. A 427 (1999) 170-176
19. J. Lettry et al., 'Ion sources for MedAustron', Rev. Sci. Instrum. 81 (2) Feb 2010, 02A328
20. R. Becker, 'Characterization of ion sources' chapter 2 / section 11 in 'Handbook of ion sources, ed. B. Wolf, CRC Press Inc. 1995, 157-182
21. E. D. Donets, 'Electron beam ion sources', chapter 12 in 'The physics and technology of ion sources', ed. I. Brown, John Wiley & Son, 1989, 245-279
22. F. Currell and G. Fussmann, 'Physics of electron beam ion traps and sources, IEEE Transactions on plasma science, vol 33(6) (2005) 1763-1777
23. R. Becker and M. Kleinod, 'Space-charge compensation of electron beams by thermal ions and the production of highly charged ions in EBIS and EBIT', Rev. Sci. Instrum. 65 (4), April 1994, 1063-1065
24. Lyman Spitzer Jr, 'Physics of fully ionized gases', Interscience Tracts on Physics and Astronomy (1962)
25. R. Becker, 'Acceleration and heating of multiply charged ions in dense electron beams', Proc. 2<sup>nd</sup> EBIS workshop, Saclay-Orsay (1981) 185-196
26. K. Reisinger, 'Emittance measurements on the sideband cooling technique and introduction of the rotating wall cooling technique at REXTRAP, Master's thesis, Technische Universität, München, 2002.
27. D. J. Heinzen et al., 'Rotational equilibria and low-order modes of a non-neutral ion plasma', Phys. Rev. Lett. No 16 (1991) 2080-2083
28. E. Kugler, 'The ISOLDE facility', Hyperfine Interact. 129 (2000) 23–42

29. A. M. Ghalambor Dezfuli, R.B. Moore, P. Varfalvy, 'A compact 65 keV stable ion gun...', Nucl. Instrum. Meth. A368 (1996) 611-616
30. L. Penescu et al., 'Development of high efficiency Versatile Arc Discharge Ion Source at CERN ISOLDE', Rev Sci Instrum. 81 (2), Feb 2010, 02A906
31. C. E. Melton and G. F. Wells, 'Dissociation of CO<sup>+</sup> and CO<sup>++</sup> ions by collision with neutral molecules', The Journal of Chemical Physics 27 (1957) 1132-1141
32. K. Blaum and F. Herfurth, 'Trapped Charged Particles and Fundamental Interactions', Lect. Notes Phys. 749, 2008, Springer Berlin Heidelberg
33. P. Delahaye, F. Ames and A. Kellerbauer, 'Study of the charge exchange process at low energy with REXTRAP', Nucl. Phys. A 746 (2004) 604c-607c
34. J. Pitters, M. Breitenfeldt and F. Wenander, 'Charge breeding of CO<sup>+</sup> beams at REX-ISOLDE', AIP Conference Proceedings 2011 (2018) 070012
35. F. Wenander, P. Delahaye and R. Scrivens, 'The REX-ISOLDE charge breeder as an operational machine', Rev. Sci. Instrum. 77 (2006) 03B104
36. E. Beebe et al., 'Reliable operation of the Brookhaven EBIS for highly charged ion production for RHIC and NSRL', AIP Conf. Proc. 1640 (2015) 5
37. A. Pikin et al., 'RHIC EBIS: basics of design and status of commissioning', 2010 JINST 5 C09003
38. H. Pahl et al., 'A low energy beam line for TwinEBIS', 2018 JINST 13 P08012
39. K. Noda, 'Beam delivery method for carbon-ion radiotherapy with the heavy-ion medical accelerator in Chiba', Int. J. of Particle Therapy, Vol. 2, No. 4 (2016) 481-489
40. F. Herfurth et al., 'A linear radiofrequency ion trap for accumulation, bunching, and emittance improvement of radioactive ion beams', Nucl. Instrum. Meth. A 469 (2001) 254-275
41. A. Ringvall Moberg, et al., 'ToF and molecular beam studies of the on-line beam with the ISOLDE RFQ beam-cooler', EMIS 2018, Nucl. Instrum. Meth. B, to be published
42. P. Delahaye, GANIL, private communication, 2011
43. R. Boussaid et al., 'Development of a radio-frequency quadrupole cooler for high beam currents', Phys. Rev. Accel. Beams, 20 (2017) 124701
44. R. Boussaid et al., 'Experimental study of a high intensity radio-frequency cooler', Phys. Rev. ST Accel. Beams 18 (2015) 072802
45. J. Powell et al., 'BEARS: radioactive ion beams at LBNL', AIP Conf. Proc. 455 (1998) 999-1002
46. W. M. Haynes, (ed.). 'CRC Handbook of Chemistry and Physics 94th Edition', CRC Press LLC, Boca Raton: FL 2013-2014, 3-344
47. A. Yu. Boystov et al., 'Electron string ion sources for carbon ion cancer therapy accelerators', Rev. Sci. Instrum. 86 (2015) 083308
48. R. Geller, 'Electron Cyclotron Resonance Ion Sources and ECR Plasmas', IOP Publishing Ltd. (1966), ch. 3.5
49. [https://indico.cern.ch/event/264020/attachments/467855/648233/SEMINAR\\_OUTGASSING-2004-06-17-PChiggiato.pdf](https://indico.cern.ch/event/264020/attachments/467855/648233/SEMINAR_OUTGASSING-2004-06-17-PChiggiato.pdf)
50. S. Stegemann, 'Production of intense mass separated <sup>11</sup>C beams for PET-aided hadron therapy', International Conference on Electromagnetic Isotope Separators and Related Topics, 2018, CERN
51. K. Katagiri et al., 'Cryogenic molecular separation system for radioactive <sup>11</sup>C ion acceleration', Rev. Sci. Instrum. 86 (2015) 123303
52. E. Benedetto. 'Superconducting synchrotron and gantry based on canted cosine theta magnets', Workshop on ideas and technologies for a next generation facility for medical research and therapy with ions, 2018, Archamps, France
53. B. Franzke, 'The heavy ion storage and cooler ring project ESR at GSI', Nucl. Instrum. Meth. B 24/25 (1987) 18-25
54. W. Bartmann et al., 'CERN ELENA project progress report', EPJ Web of Conf. 95 (2015) 04012
55. J. Bossler, et al., 'Experimental investigation of electron cooling and stacking of lead ions in a low energy accumulation ring', Particle Accelerators 63 (1999) 171-210
56. S. Verdú Andrés et al., 'CABOTO, a high-gradient linac for hadrontherapy', J. Radiat. Res. 54 (suppl 1) (2013) 155-161
57. S. Benedetti, 'High-gradient and high-efficiency linear accelerators for hadron therapy', PhD thesis 2018, Lausanne, EPFL, [https://infoscience.epfl.ch/record/253063/files/EPFL\\_TH8246.pdf](https://infoscience.epfl.ch/record/253063/files/EPFL_TH8246.pdf)
58. 'Strategy and Framework Applicable to Knowledge Transfer by CERN for the Benefit of Medical Applications', CERN/SPC/1091, 2017

59. R. Mertzig et al., 'A high-compression electron gun for C6+ production: concept, simulations and mechanical design', Nucl. Instrum. Meth. A 859 (2017) 102-111
60. M. Breitenfeldt et al., 'MEDeGUN commissioning results', AIP Conf. Proc. 2011 (2018) 040004